MONASH MOTORSPORT

FINAL YEAR THESIS COLLECTION

Development and Design of a Formula SAE Exhaust System

Reece Day - 2020

The Final Year Thesis is a technical engineering assignment undertaken by students of Monash University. Monash Motorsport team members often choose to conduct this assignment in conjunction with the team.

The theses shared in the Monash Motorsport Final Year Thesis Collection are just some examples of those completed.

These theses have been the cornerstone for much of the team's success. We would like to thank those students that were not only part of the team while at university but also contributed to the team through their Final Year Thesis.

The purpose of the team releasing the Monash Motorsport Final Year Thesis Collection is to share knowledge and foster progress in the Formula Student and Formula-SAE community.

We ask that you please do not contact the authors or supervisors directly, instead for any related questions please email info@monashmotorsport.com

DEVELOPMENT AND DESIGN OF A FORMULA SAE EXHAUST SYSTEM

SUMMARY

This project includes a broad range of work and various investigations in the pursuit of improving the understanding of and techniques involved in designing and fabricating a high-performance Formula-SAE/Formula Student exhaust system.

A stainless steel manifold and two double-pass absorptive mufflers were designed, manufactured and tested. The effect of various exhaust geometries on system back-pressure and noise results were investigated, along with the effect of an argon purge on weld quality. Major material failures are documented, as well as the nature of the degradation of absorptive material in the mufflers. This report also contains some details on avenues of study which were unable to be completed due to resource limitations or the COVID-19 outbreak.

The major outcomes of this project are:

- A high-performance FS/FSAE exhaust system was successfully designed and implemented.
- The double-pass design of the muffler is justified by conclusive back-pressure testing results.
- Back-pressure testing reveals a relationship of approximately 0.55 competition points per kPa of pressure.
- The outlet direction is justified by noise test results, and outlet geometries validated by these tests are implemented on the vehicle.
- A low-budget argon purge system is fabricated and tested, resulting in limited effectiveness depending on the nature of the weld.
- The rate of packing material ejection/loss from the muffler is investigated but the results are inconclusive due to a small sample size.

TABLE OF CONTENTS

1. INTRODUCTION

Formula SAE, or Formula Student as it is known in Europe, is the world's largest engineering design competition. It involves hundreds of completely student-run teams from universities around the world who design, build, test and compete with formula-style race cars. The competitions are judged based on a "points" system over multiple events; a vehicle which performs better at an event will score more points, up to a maximum of 1000, leading to a better ranking overall at that competition. The vehicles are also subject to an extensive and strict set of rules regarding construction or limits, such as roll cage specifications and a noise limit for internal combustion-powered vehicles.

Monash Motorsport ("MMS") is Monash University's Formula SAE team, and their internal combustion car is named M20-C, a continuation of the vehicle previously called M19-C in 2019. The car utilizes a naturally aspirated KTM Duke-R 690cc single cylinder-engine. Monash Motorsport strives to become the most respected formula SAE team in the world. by continually improving their performance to the highest standard, and this Final Year Thesis endeavours to achieve this.

The overall aim of this project is to refine the design and manufacturing techniques of the exhaust system of the M20-C. This will provide future designers with information which will assist in the continuous improvement of the exhaust system, through the investigation of multiple avenues of potential development. The ideal exhaust system would maximise engine performance, minimise mass, and stay within an acceptable budget.

The objectives of this project as originally stated in the Project Proposal, in order of priority, are:

1. To design exhaust systems for the 2019 and 2020 season with the maximum points potential possible with the team's resources.
2. To improve the accuracy of Monash Motorsport's exhaust "points delta" design philosophy.
3. To provide an improved groundwork of test results to allow future exhaust designers at MMS to create reliable and high-performance systems with minimal speculation or estimation of system parameters.

2. SYSTEM DEVELOPMENT

2.1 Back-pressure Study

In a naturally aspirated engine, such as the one used by MMS's M20-C, the engine must act as its own air pump. For air to flow from the atmosphere into the intake manifold, the intake manifold must be below atmospheric pressure. For exhaust gases to flow out of the exhaust manifold, the exhaust must be above atmospheric pressure. Thus, the engine must push air from a low-pressure manifold into a high-pressure one. This process takes work out of the engine's thermodynamic cycle in the form of the pumping loop, and the greater the pressure difference the more energy is used, and therefore the engine produces less net power. In steady-state, the exhaust manifold will have reached an equilibrium pressure difference/drop along its length which drives the flow necessary to move the amount of gas produced by the engine. This pressure above atmospheric is colloquially known as "back-pressure", as restriction in the exhaust causes pressure to "back up" against the engine's exhaust valve(s). Due to the cyclic nature of an internal combustion engine, the exhaust

manifold will never be in steady-state, but an equivalent nominal/average level of back-pressure can be measured. An exhaust system will reach higher levels of back-pressure when the engine operates at a higher RPM since the engine pumps more gas as it cycles faster.

For many years, MMS has been using a “straight-through”/single-pass absorptive muffler in order to reduce exhaust noise levels below the allowed maximum. It has long been observed on the team that reducing the diameter of internal geometry or the outlet of a muffler reduces noise. The single-pass mufflers required outlet tube diameters of 1 inch (25.4mm) in order to be effective in 2018 and prior, as shown in Figure 1. However, recent changes to the way noise is measured at the Australasian competition from 2019 onwards would require the outlet to be reduced to 0.5 inch (12.7mm) in order to pass the noise test. In a previous study undertaken by an MMS exhaust engineer, such single-pass mufflers were found to produce approximately 40kPa of back-pressure, and reducing the size of the outlet could increase back-pressure by up to 90kPa (Boneh, 2016). In this study it was also found that despite the increase in back-pressure, the car’s lap times were only reduced by 0.4%.

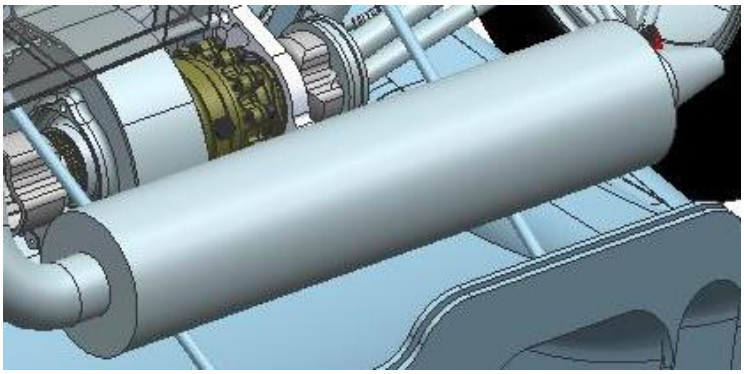

Figure 1: CAD screenshot of single-pass absorptive muffler with reduced outlet (Boneh, 2016).

Early in this project, it was theorised that the car would benefit from a double-pass muffler design; the increase in absorptive volume would allow for the nominal size of internal geometry to be increased compared to the single-pass muffler design. This would reduce the pressure drop across the system and thus increase potential engine power. A stainless steel double-pass prototype muffler was therefore manufactured for testing. It is similar to the design shown in Figure 9, except with only a 300mm-long absorptive section. In order for this design to pass the noise test, it required a 1 inch reducer on its outlet.

The exhaust manifold was designed with a threaded boss welded into it to allow for the connection of a pressure sensor. This boss was kept plugged for most of the year, but a pressure sensor was fitted and used to test seven exhaust configurations in a testing session early in the project. The pressure sensor used was a Honeywell PX3 series sensor, which measures absolute pressure and is rated to a maximum temperature of 125°C. Since the exhaust temperature is much higher, the sensor was fitted to the exhaust manifold via a long copper pressure tap tube to isolate it thermally, as shown in Figure 2.

At this stage of the project, M19-C was unavailable and thus the test was performed on M18-C, which has the same engine and a very similar exhaust manifold. The car drove multiple laps with each configuration on a track with a combination of turns and straights often seen in Formula Student/SAE competitions.

Figure 2: Pressure tap tube and sensor attached to the M18-C's exhaust manifold.

Figure 3 is the summary plot of the nominal peak back-pressure each tested muffler/configuration produced, and the corresponding peak power the engine was able to produce. The "nozzles" are reducers attached to the exhaust pipe in place of a muffler. They are not competition-legal exhaust configurations, and only serve the purpose of providing additional data points on this graph in order to assist in the estimation of a relationship between back-pressure and engine power. The single-pass muffler with a 1 inch outlet is used as the control for the purpose of these tests, as it was MMS's most popular design historically. It can be seen that there is a weak trend showing that less back-pressure corresponds to more power. The small sample size of six configurations on this graph make it difficult to draw a conclusive relationship, but if it is assumed to be linear for this range of pressures, then the engine power is inversely proportional to the back-pressure by a factor of 0.22. According to MMS's competition points simulator, there is a difference of 11.58 points at competition for every 10% change in engine power. In this power range, that is approximately 2.5 points per kilowatt of power. Combing these factors, we find the resulting ratio of 0.55 points/kPa of back-pressure.

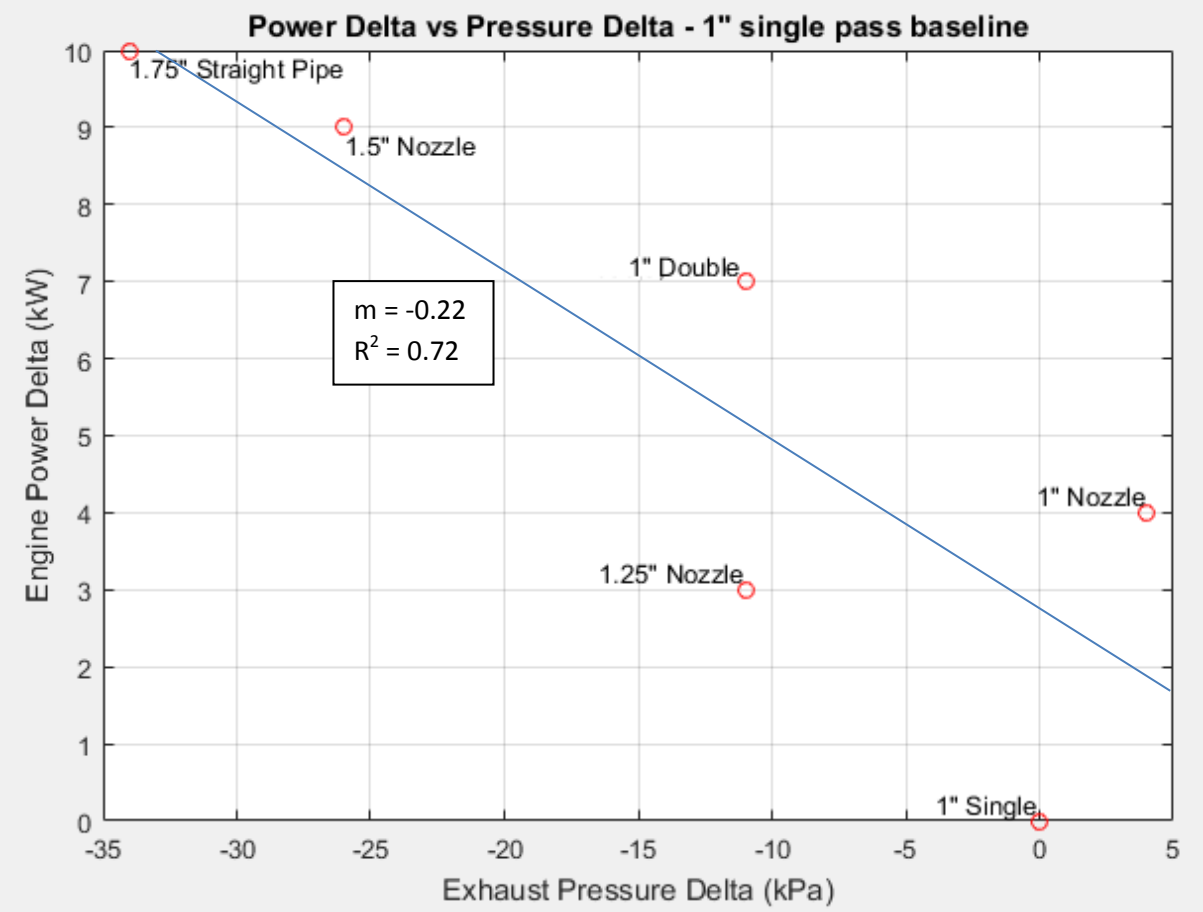

Figure 3: "Power Delta vs Pressure Delta" plot showing the approximate relationship between differences in nominal peak exhaust back-pressure and the difference in the engine's peak power.

The single-pass muffler with the 0.5 inch outlet was also tested, but caused more than 2.5 times as much back-pressure as the 1 inch outlet. It was excluded from the above plot to avoid distorting the scale for readability.

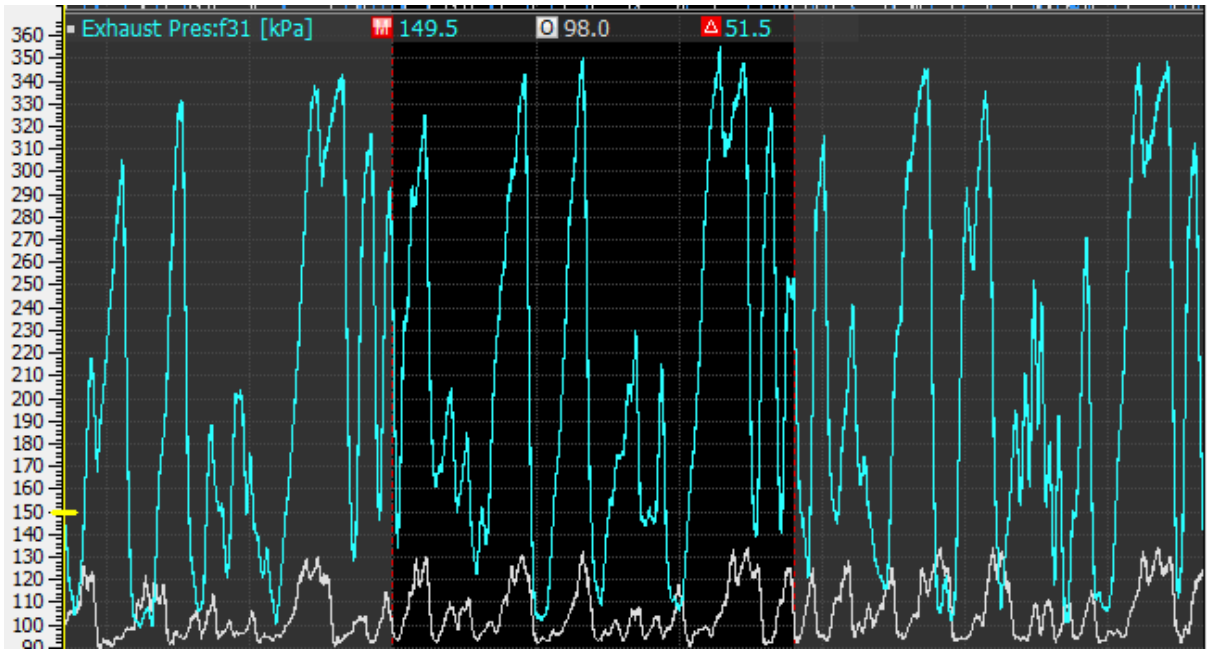

Figure 4: MoTeC trace of exhaust back-pressure over 3 laps of the test track. Grey: 1 inch outlet muffler. Blue: 0.5 inch outlet muffler.

Figure 4 below is a plot of exhaust pressure in kPa over time. The two traces are lined up so they each correspond to the same sections along the test track. The blue trace is the 0.5 inch outlet and the grey is the 1 outlet. It is clear that the reduced outlet size increases back-pressure significantly. The barometric pressure was not recorded on the testing day, but atmospheric pressure typically fluctuates by only 2-3kPa in the area (Clayton, Victoria). The test track is at an altitude of 70 meters above mean sea level, so atmospheric pressure on the day was likely around 100kPa. The back-pressure sensor recorded a pressure level as low as 90kPa in the "troughs" of the pressure trace as shown in Figure 4, which is when the engine is operating at a low RPM and thus not producing enough gas to cause back-pressure to build up. Therefore, it is possible that the pressure sensor was miscalibrated, or not zeroed correctly. The 1 inch outlet single-pass muffler, which is almost the same as the design shown in Figure 1, produces about 40kPa of peak-to-peak back-pressure (90kPa to 130kPa) each time the engine is operated at high RPM for a long enough time. This value correlates with Yuval Boneh's findings (Boneh, 2016) that a single-pass muffler produces 40kPa of back-pressure. The 0.5 inch outlet caused the minimum (trough) pressure level to be increased by about 10kPa and the peak-to-peak back-pressure increases to up to 250kPa.

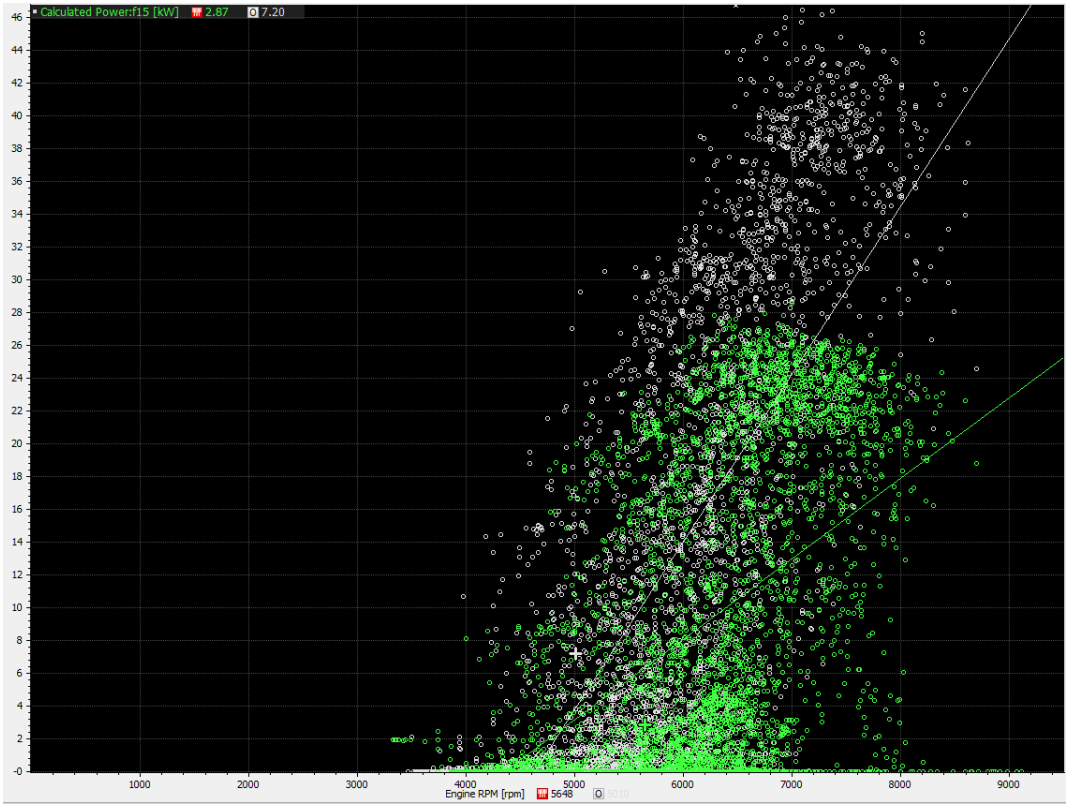

Figure 5: MoTeC scatter plot of engine power vs. engine RPM. Grey: 1 inch outlet muffler. Green: 0.5 inch outlet muffler. Notice the drastic difference in peak engine power.

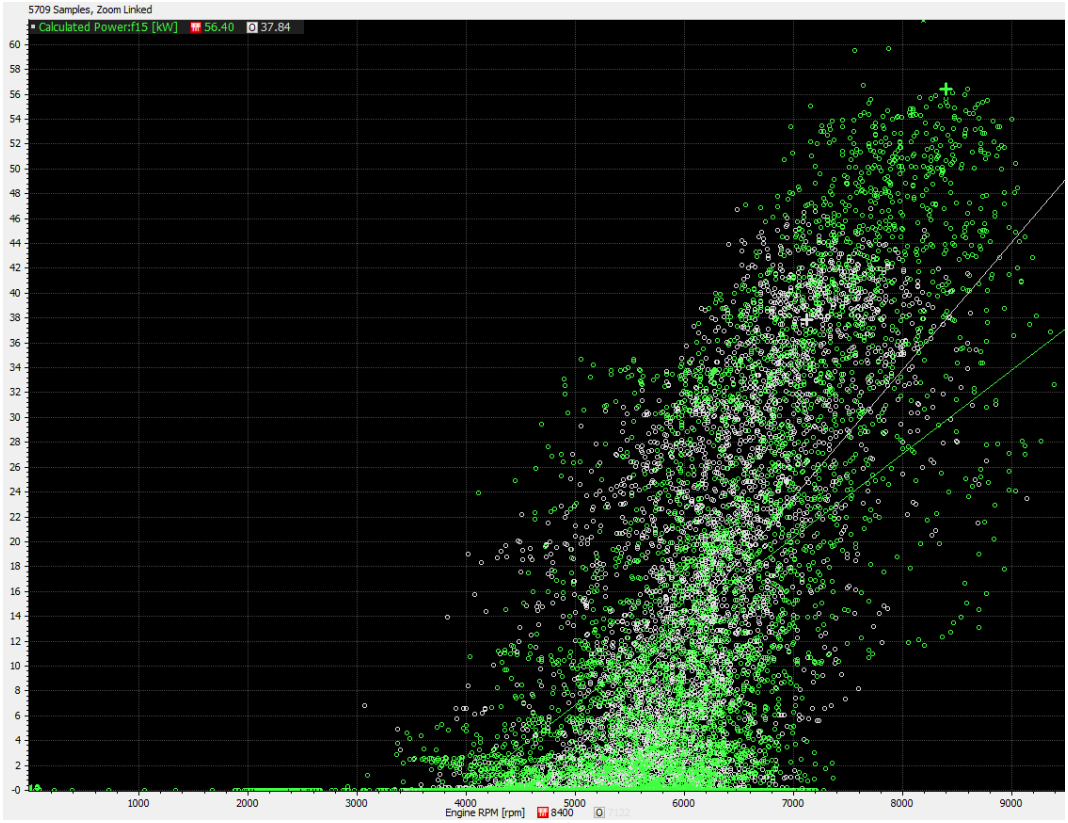

Figure 6: MoTeC scatter plot of engine power vs. engine RPM. Grey: 1 inch outlet muffler. Green: Unrestricted "straight pipe" exhaust.

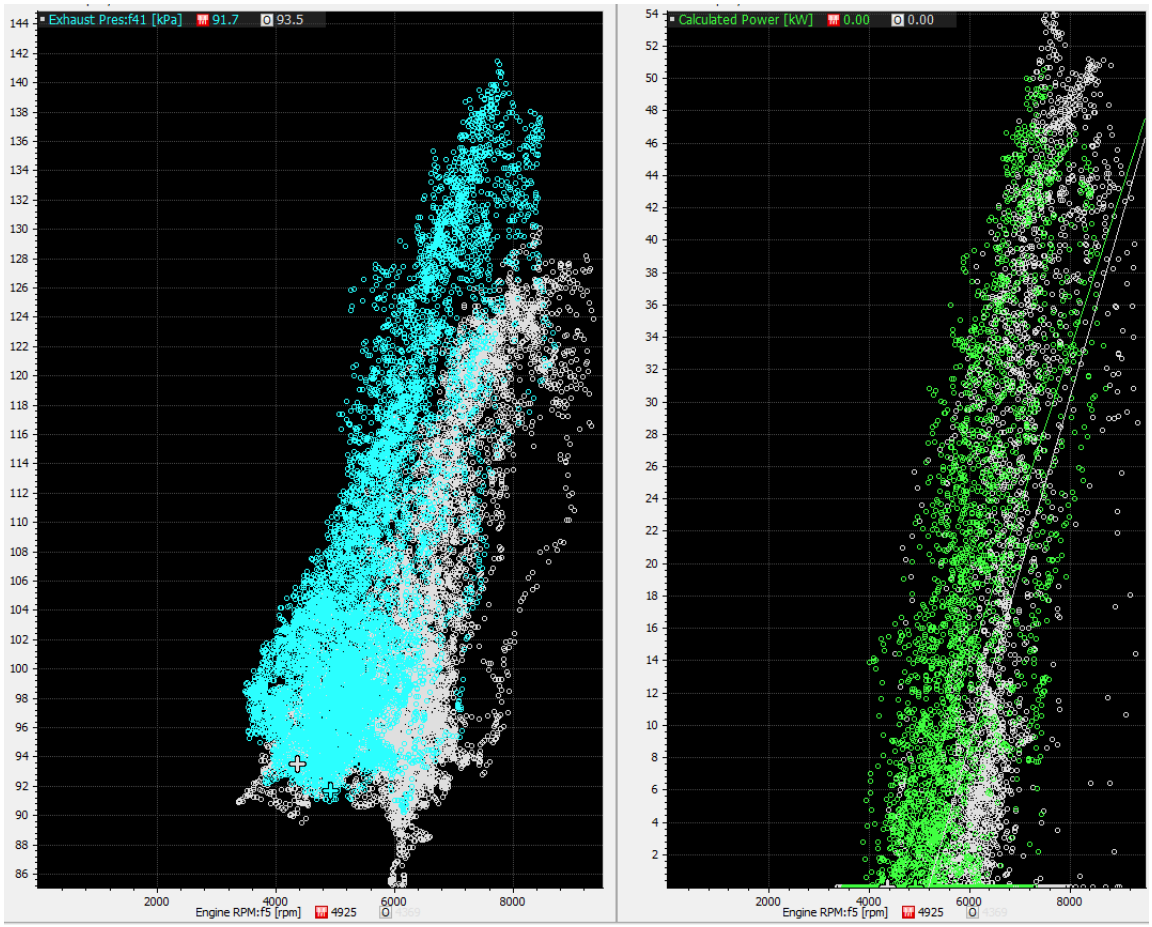

Figure 7: Left: Scatter plot of back-pressure vs. engine RPM. Right: Scatter plot of engine power vs. RPM. Green & Blue: Single-pass muffler. Grey: Double-pass muffler.

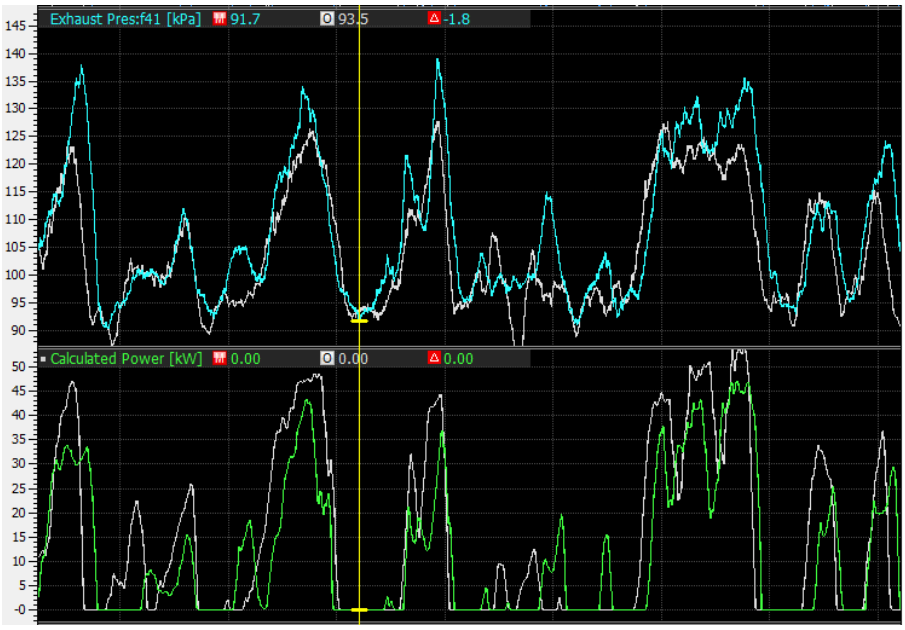

Figure 8: Top: Trace of back-pressure over a lap of the test track. Bottom: Trace of corresponding engine power through the test track lap. Green & Blue: Single-pass muffler. Grey: Double-pass muffler.

Figure 5 is a scatterplot of engine power against engine RPM for the same mufflers, showing a difference of about 18kW in peak power. With a competition points sensitivity of 11.58 competition points per 10% change in engine power, this means that the 0.5 inch outlet has a points delta of -45 compared to the 1 inch tip. This is a highly significant difference. The car was noticeably sluggish during the test with this highly restrictive muffler attached.

Figure 6 is a similar power vs RPM plot, this time comparing the 1 inch single-pass muffler and "straight pipe", meaning no muffler or device at all. The unrestricted exhaust allows the engine to produce 10 extra kW, equivalent to approximately 25 competition points. This is essentially the theoretical maximum power the exhaust manifold could allow the engine to produce, but in practice it is impossible to pass the noise test without at least some restriction. This demonstrates how far from "perfect" any particular future exhaust design is.

Figure 7 and Figure 8 compare the prototype double-pass muffler with the single-pass muffler. Although they have the same outlet size, the double-pass muffler generates less back-pressure. This could be due to its larger capacity providing more space to store excess gas in a capacitive fashion, or from gas bypassing the end-chamber and moving through the fibreglass absorptive material. The double pass design allows the engine to produce about 7kW of extra power. In MMS's competition points simulator, 1kg of mass makes a difference of 1 point. Therefore, the double-pass design results in a +16 competition points delta compared to the 1 inch single-pass design used previously, including the loss of 1.5 points due to a 1.5kg increase in mass. And it provides a +71 points delta compared to the 0.5 inch outlet single-pass muffler, which is the size of outlet required for that muffler to meet the new noise limit rules at the FSAE-A competition. Therefore, it was decided that the M19-C and M20-C would utilise a double-pass muffler design.

2.2 Mild Steel Muffler Manufacture

A new double-pass muffler was designed, and was to be made from stainless steel. Figure 9 shows a CAD cross section of the design, along with some nomenclature used to describe components of the muffler. The prototype double-pass showed that trading additional mass for larger tube sizes was beneficial, so this new muffler would go one step further and have a 1.5 inch outlet. The absorptive length was increased to 500mm to compensate for the associated increase in noise level.

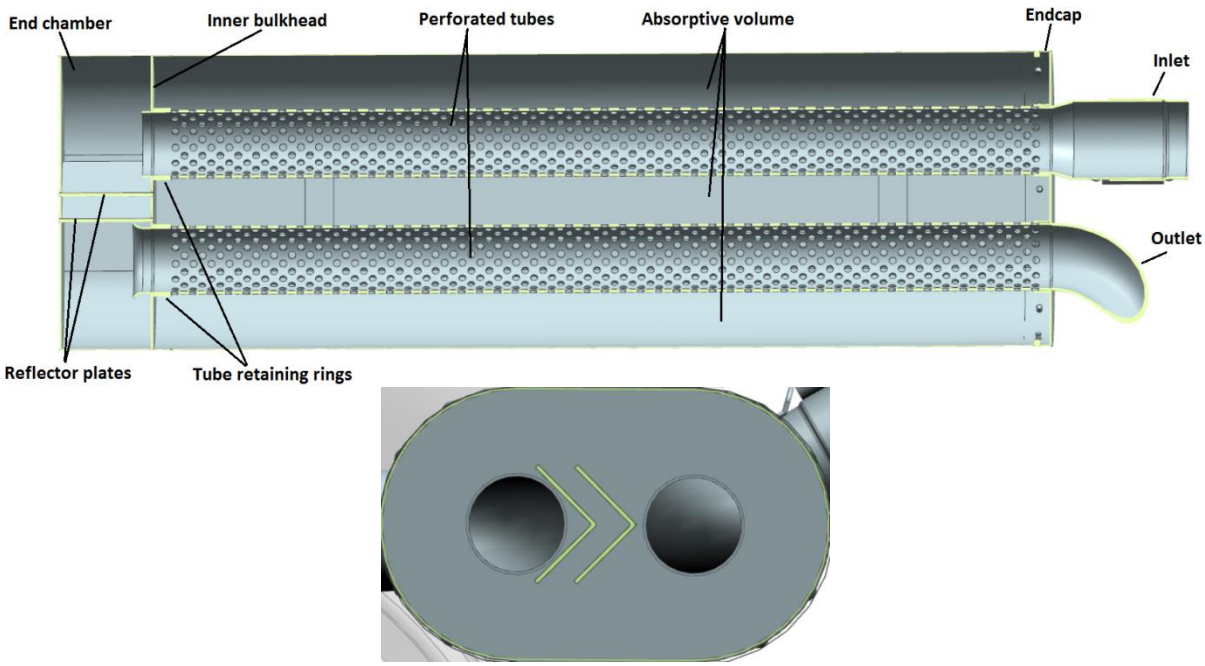

Figure 9: Top: Cross section of double-pass muffler design. Bottom: Cross section of end chamber, showing central reflector plates which help reduce noise transmitted through the chamber.

Due to resource constraints, an interim design comprised of mild steel was manufactured and proved to be a useful test/prototype for manufacturability and fabrication methods. A pill-shaped cross section was chosen in order to keep a constant distance between the internal perforated tubes and the case. Pieces such as the case and bulkheads were laser cut, and then the case was manually rolled on a sheet metal roller as shown in Figure 10.

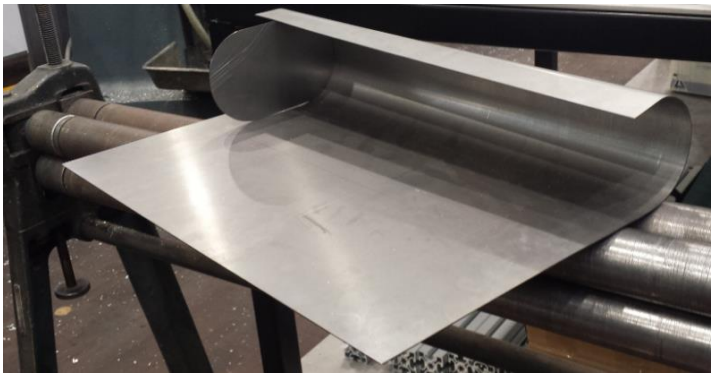

Figure 10: Mild steel muffler case and bulkhead resting on Monash University Mechanical Engineering Technical Services' sheet metal roller.

The end chamber of the muffler includes two short lengths of tube protruding into its volume at its inlet and outlet, as such geometry has been shown to increase the acoustic transmission loss in hollow silencers, as seen in Figure 11 (Beranek, 1988). This affects different frequencies by different amounts, depending on the exact geometry, but on average the transmission loss is higher overall compared to a non-protruding inlet and outlet.

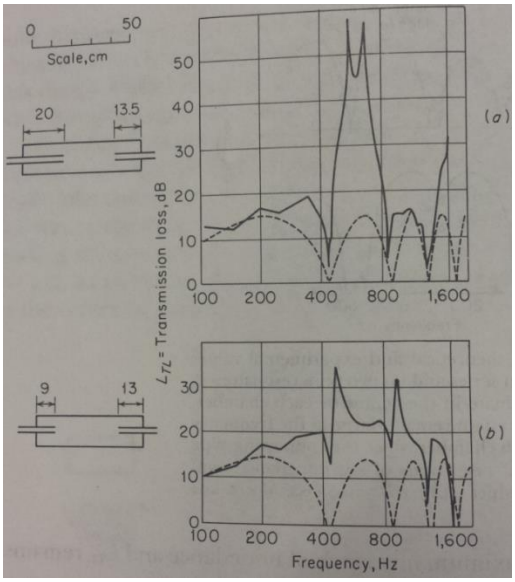

Figure 11: Frequency spectrum transmission loss of hollow chambers with protruding inlets and outlets (Beranek, 1988). Solid lines are with protrusions, dotted lines are without.

The end chamber also includes two chevron-shaped plates which block line-of-sight between the inlet and outlet, forcing exhaust gas to move around the outside of the chamber. The channel between these two plates also directs pressure waves from each side of the chamber to the other, causing destructive interference. The design is inspired by the "Delta plates" used in a particular FlowMaster brand muffler, shown in Figure 12 below (Kimbrough, 2014). Angling the plates away from the inlet as in the FlowMaster muffler may improve flow characteristics, but the double-pass muffler's end chamber design has the two plates facing the opposite direction, as the concave shape may improve transmission loss by reflecting incident sound waves back towards the inlet.

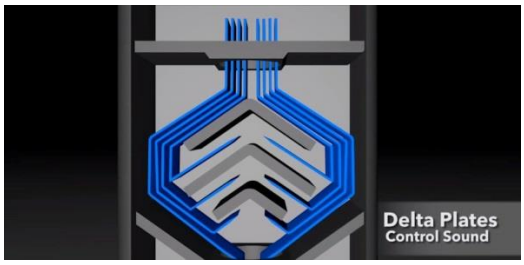

Figure 12: "Delta Plate" technology in a FlowMaster muffler (Kimbough, 2014), showing how some noise (blue lines) are directed into channels between the plates.

The opposite side of the inner bulkhead also includes lengths of tubes which locate and hold the perforated tubes in the adjacent absorptive section. These 6 small components were all welded to the inner bulkhead as shown in Figure 13, then that bulkhead was welded to the chamber case as shown in Figure 14.

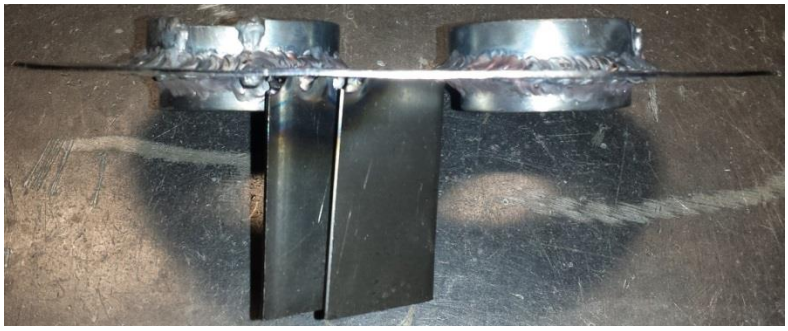

Figure 13: Mild steel inner bulkhead with inlet and outlet tubes, retaining rings, and reflector plates. The outer bulkhead was then tack-welded to the other end of the reflector plates.

Figure 14: Mild steel end chamber assembly being inserted in the end chamber case prior to welding.

After welding the finished end-chamber to an open end of the rolled main case, the case was welded closed with a seam along its length. To ensure the case stayed in the correct shape, a spare bulkhead was inserted inside and the case was tightened around it with a hose clamp as shown in Figure 15. After the weld cooled and the jig was removed however, the case had still warped inward from the weld as shown in Figure 16. This was easy enough to fix with manual hand-bending techniques since the mild steel is easily pliable.

Figure 15: Spare bulkhead and hose clamp being used to shape/jig muffler case prior to welding.

Figure 16: Mild steel muffler internal view prior to packing and endcap attachment.

To make the endcap, a bulkhead with inlet and outlet holes was welded to a 15mm-wide strip of steel which is bent to match the shape of the case. This endcap is then riveted to the main case. The ends of the strip were welded together in order to close the loop formed by the bent strip. To ensure a good seal with the case, it was important that the weld bead did not come through to the inside of the endcap. This was almost successful, but unfortunately one small bump had to be filed back. The bump was up against the back wall of the bulkhead as shown in Figure 17, which restricted tool access. A small powered Dremel-style grinding tool removed the bump quite easily however.

Figure 17: Weld penetration on the underside of the endcap strip. Penetration is undesirable for this particular weld, and the bead near the back had to be removed for the endcap to seal.

The muffler is mounted laterally near the rear of the car, and originally the muffler's outlet was to make a 90° turn immediately upon exiting the second absorptive pass and face the rear of the car, this being the safest place to exhaust the hot gases. However, the outlet had to be extended in order to avoid interference with the car's heat-sensitive undertray. The unpainted extension is shown in Figure 18. Also in Figure 18 is a pie-cut 90° outlet tip which was used to test the effect of pointing the outlet to the side of the car. It was found that noise level is reduced greatly by pointing the outlet sideways, so the outlet was modified a second time to remove the 90° bend, as shown in Figure 19. Details of these noise tests are presented in section 2.6 of this report.

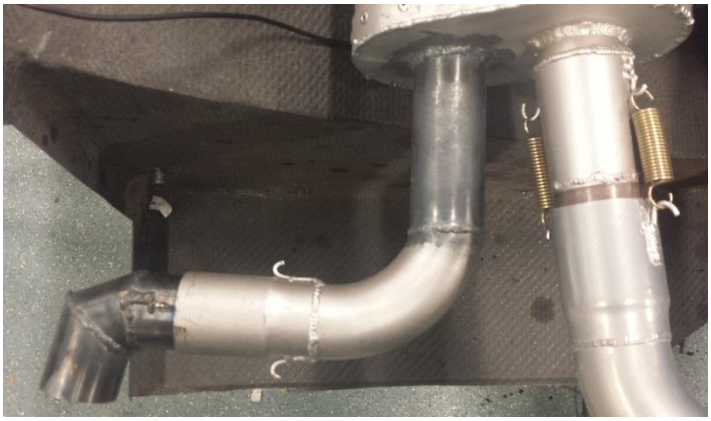

Figure 18: The mild steel muffler's extended rearward outlet, and 90° outlet tip connected via slip joint.

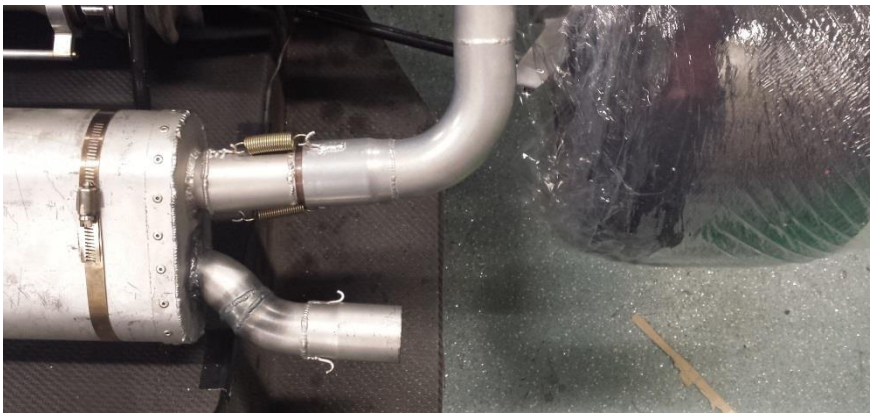

Figure 19: The mild steel muffler's side-facing outlet after further modification.

The muffler was painted with silver high-temperature paint for aesthetics. The final mild steel muffler, after a few hundred kilometres of testing, is shown in Figure 20. The outlet is 150mm long, the end-chamber is 50mm long and the absorptive section is 500mm long, providing 1m total length of perforated tube interfacing with the absorptive volume of 5768.9cm^3 and a total muffler length of 700mm. It weighs 3507g without fibreglass and a nominal 4875g with glass, using approximately 1368g of glass with each repacking. It reduced noise to 6dB under the limit and therefore the next iteration, the stainless steel muffler, had its absorptive section reduced to a length of 450mm in order to reduce mass.

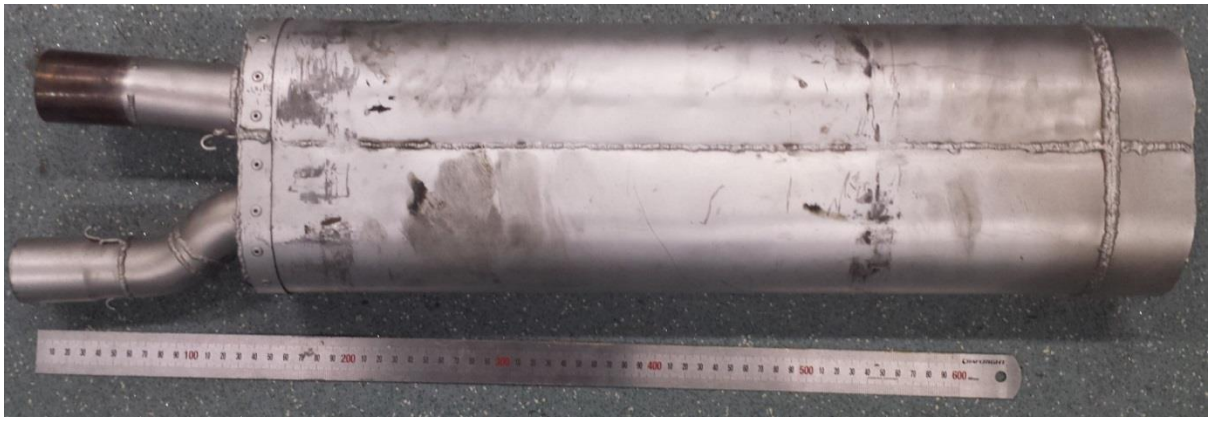

Figure 20: The finished mild steel double-pass muffler.

2.3 Argon Purge System

Prior to welding the stainless steel exhaust manifold and muffler, a system which allows for the back side of welds to be purged with argon gas was developed. The motivation for this is that the inclusion of oxygen or nitrogen in welds causes poor weld quality and fusion, and is why TIG welding involves argon gas being constantly pumped around the electrode to cover the weld pool. On thin metal or full-penetration welds however, the back side of the material is hot enough to react with the atmosphere as well. For tube welds or welds on "enclosed" objects/shapes, the part itself can be filled with argon. Purging parts which don't form an enclosed space requires submersing them in a tank or container of argon. Expensive versions of these tanks are air-tight and the user must manipulate the welder via gloves sealed into the walls, such as the example shown in Figure 21 below (RCW Aerospace Specialist Welding Solutions).

Figure 21: A technician operating a sealed welding chamber (RCW Aerospace Specialist Welding Solutions).

However, a cheaper, version of these argon tanks involves having an open top, and constantly providing argon from the bottom of the tank in order to keep it under positive pressure relative to the atmosphere. Since argon is heavier than air, the tank would fill with the invisible gas and the positive pressure would then cause it to flow over the edges and down the outside of the walls. An argon purge tank was made as per the diagram shown in Figure 22, and Figure 23 shows photos of the finished box with a plywood lid. The design is inspired by a similar box demonstrated on the popular Youtube channel "weldingtipsandtricks" (Collier, 2016). The argon is fed into a hollow chamber at the bottom, and then filters up through stainless steel wool which helps disperse the argon evenly and reduce turbulence in the gas flow. The wool is held up by a perforated steel sheet which is held in place by small shelves riveted to the wall.

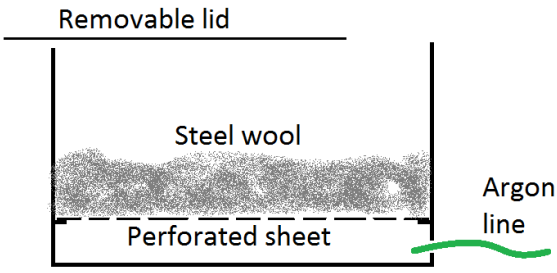

Figure 22: Diagram of basic argon purge tank design.

Figure 23: Left: Argon hose inserted into bottom section of tank. Right: Argon purge tank with lid open.

To test the box, a mock-up of the end-chamber inner bulkhead welding arrangement was made from scrap pieces of stainless steel sheet. The bare stainless steel wool proved to be an ineffective material to electrically ground the part, so the part was placed on solid metal billets to establish solid grounding, as shown in Figure 24.

Figure 24: Stainless steel inner bulkhead mock-up resting on spare billets in the purge tank.

The first test was a control test without argon purge. The result includes a lot of “sugaring”; the formation of crystals of chromium carbide and oxide on the back side of welds, as shown in Figure 25. The sample is also heavily straw coloured. In addition to the oxidation, the sample experienced extensive thermal warping.

Figure 25: Resulting welds from unpurged control test in the purge tank. Note the excessive discolouration and warping, caused by the poor access conditions when welding over the walls of the tank.

In order to reduce thermal warping, the following tests were performed with the sample pieces clamped to a sheet of aluminium with small clamps and aluminium blocks, as shown in Figure 26.

Figure 26: A stainless steel fillet weld jigged onto an aluminium sheet, inside the purge tank.

In this test shown above in Figure 26, the tank was purged with argon gas. The presence of argon was confirmed by slowly submerging a naked flame into the tank. As the flame went below the level of the walls and entered the tank's volume, the flame was extinguished. Comparisons of results between samples with and without an argon purge are shown below in Figure 27 and Figure 28. It was observed that the presence of argon completely eliminated the crystallisation of the stainless steel, and greatly reduced oxidation. The purged weld still had some discolouration, especially near the heat-affected zone of the welds. High-purity argon was used (10 ppm contaminant gas) so this presence of oxygen could have been due to mixing of the gas through the open top of the tank.

Figure 27: Left: Underside of purged weld. Right: Underside of unpurged weld. Note the difference in colouration and crystallisation.

Figure 28: The two welded samples. Note the brighter colour of the purged sample in the foreground.

Access to the parts inside the purge chamber is made much more difficult due to the walls of the tank. This necessitates less ideal angles and positions of the torch and filler rod, which in turn causes poor weld quality. The odd and difficult angles and poor visibility usually caused welds to take more time or for higher welding current to be applied in order to create proper fusion between the pieces. This causes the welds to become overheated and also creates larger beads with more filler material than would normally be necessary. To test this and compare weld quality to a weld made with good access, another sample was set up with the aluminium sheet, blocks and clamps, but the sample was welded on an open table with no argon tank, as shown below in Figure 29.

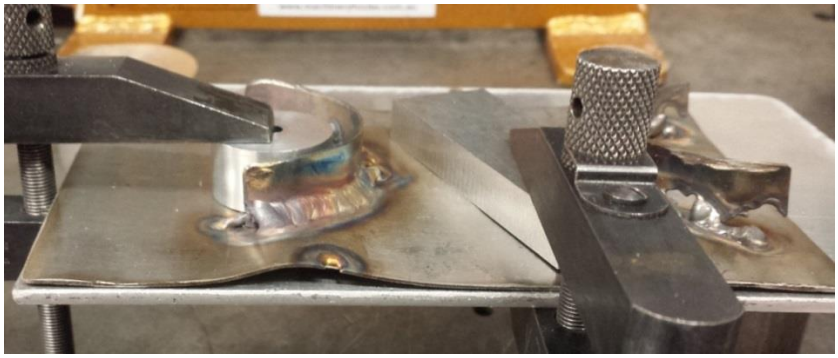

Figure 29: A stainless steel fillet weld test, jigged to an aluminium plate and welded in the open. Disregard the unrelated weld on the right; only the left-hand weld is relevant to this test.

The underside of this weld is shown below in Figure 30. Note the lack of any crystallisation. The sample also shows less discolouration from oxidation than the purged sample in Figure 27. This shows that clamping the part to a solid aluminium sheet is more effective at blocking the atmosphere's access to the back side of the weld than attempting to replace the atmosphere with argon. The aluminium also acts as a heat sink which helps keep heat concentrated to the weld pool and reduces the spread of heat across the part, which also acts to reduce oxidation. However, the back side of the weld which is not in contact with the aluminium sheet still experiences oxidation and crystallisation as shown in Figure 31. However, due to the easier access to the weld, the bead is able to be kept small and the weld is completed quickly and with ideal torch and filler rod angles, thus reducing total heat and the resulting extent of crystallisation is considered acceptable. Thus, it is concluded that for mostly-flat parts such as the muffler bulkheads, clamps and scrap aluminium are much more effective measures for improving weld quality than the argon purge tank used.

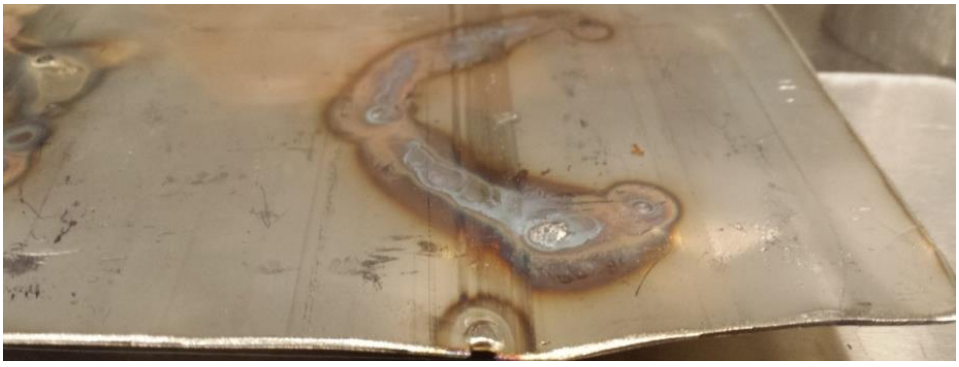

Figure 30: Underside of unpurged, clamped weld.

Figure 31: Back side of unpurged, clamped weld.

The purge system was also used without the tank to test purge effectiveness in tube welds. Since a tube is self-enclosing, the purge line is simply inserted into one end of the tube and the other end is taped over in order to reduce the amount of argon flow required to keep the tube under positive pressure by the argon line. A few small holes are made in the tape in order to provide some pressure relief when the weld seam closes, and to ensure the constant flow of argon through to the end of the tube. Ideally, an argon purge system would make use of a dual regulator, which allows the precise control of gas flow through two separate argon hoses. However, these specialised regulators are expensive. To reduce costs, a brass T-piece fitting was inserted into the TIG welder's argon hose. This simply split the argon supply between the welder hose and the purge hose, both of which are supplied with the same pressure. Therefore, the total flow is set by the single regulator, and the ratio of flow between the purge line and the torch line is determined by the ratio of flow resistance between the two lines. A completely open purge line was found to rob the torch of almost all argon flow. So a restricting plug was machined and inserted into the end of the purge line. The plug had a 1mm drilled hole and did cause more argon to flow through the torch, but still not enough. A smaller drill bit was not available, so the 1mm hole was partially closed over by striking near its opening with a centre punch four times. The resulting hole was barely visible, and created enough restriction to allow the system to work. The plug is shown in Figure 32, and the setup at each end of the tube is shown in Figure 33.

Figure 32: Argon restrictor plug with <1mm hole.

Figure 33: Left: Argon hose inserted in stainless steel tube, after removal of tape used to seal it. Right: Opposite end of the tube, showing punctured tape which prevents air from entering the tube.

The inside of an unpurged control test is shown to the right in Figure 34. Note the extensive sugaring/crystallisation. The result of the purged tube is presented in the same figure on the left, which shows no sign of crystallisation. Figure 35 shows the outside of the two welds. The unpurged sample has more discolouration on the outside. This is unlikely due to the lack of purge system, but rather due to the weld being closer to the edge of the tube and therefore retaining more heat. Regardless, it was concluded that the purge system is effective at improving weld quality in stainless steel tube welds and eliminating the formation of obtrusive crystals on the inside of the exhaust manifold.

Figure 34: Left: Purged tube weld. The dark crescent is due to misalignment of the two tubes. Right: Unpurged tube weld. Note extensive crystallisation typical of unpurged exhaust welds in MMS's past.

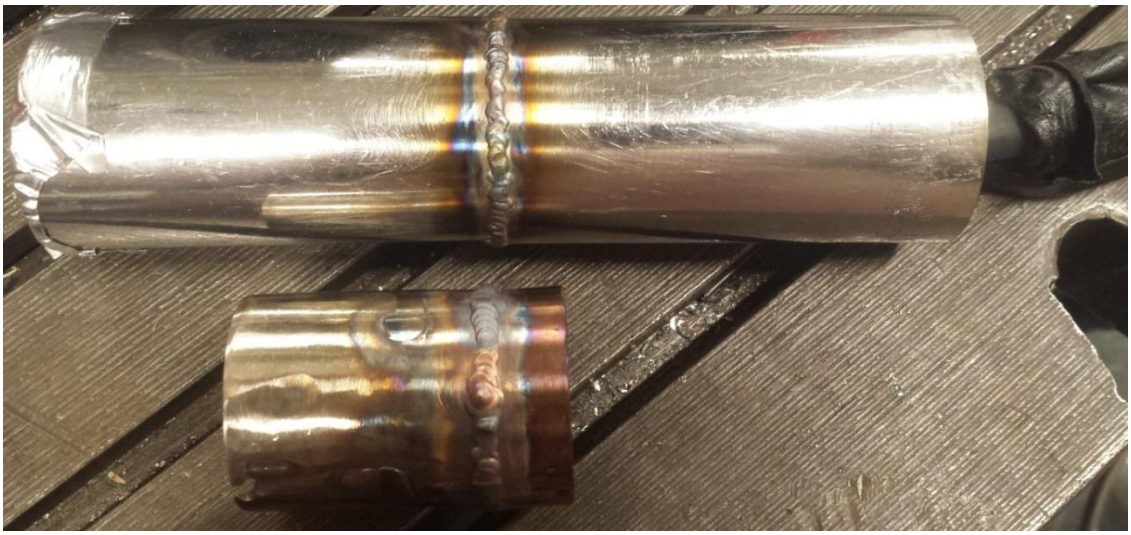

Figure 35: Outside of the purged (top) and unpurged (bottom) tube welds.

2.4 Manifold Manufacture

M19/20-C uses a single-cylinder engine with a single exhaust port, so the exhaust "manifold" is really a single tube with no collectors. It does include a number of bends, 6 mounting tabs for a heat shield, a flange and seal at the engine side and a female slip join at the muffler side. It also includes threaded bosses for a pressure sensor and an oxygen/lambda sensor. The tube was welded using the argon purge line, and there is no visible crystallisation or oxidation on the inside of the welds, as shown in Figure 36. The manifold is shown after welding in Figure 37 and after ceramic coating and mounting the heat shield in Figure 38.

Figure 36: The inside of one of the manifold's welds. Note the lack of any crystallisation.

Figure 37: Fully welded stainless steel exhaust manifold for the M19-C and M20-C.

Figure 38: Stainless steel exhaust manifold after ceramic coating. The heat shield is mounted onto spacer prongs with a plastic cable tie in this photo, but it is swapped for a steel tie before installation on the car.

2.5 Stainless Steel Muffler Manufacture

Once the stainless steel sheet arrived, work on the final muffler design could begin. The mild steel version encountered very few issues, so the stainless steel version was made in much the same way, starting with the end chamber. The stainless steel sheet is 0.02 inch (0.5mm) thick, MIL-S-5059 (AMSS518), half-hard 301 temper stainless steel sheet. It was very difficult to weld due to its tendency to "blow through" with very little heat, especially near edges. To reduce thermal warp, the end chamber was welded in "stitch" sections, evenly around the assembly, in order to spread out the heat input. Figure 39 shows the end chamber half way through welding, and Figure 40 and Figure 41 show the end chamber after finishing.

Figure 39: Partially welded stainless steel end chamber showing the intermittent style of weld seams.

Figure 40: Welded and finished stainless steel end chamber, top view.

Figure 41: Welded and finished stainless steel end chamber. Left: isometric view. Right: Side view.

After gaining experience in welding the 0.5mm sheet for the end chamber, is was decided that welding a seam down the length of the main case as was done with the mild steel muffler would be infeasible in the stainless steel version. Instead, the case was joined by folding a hook/lip into the two edges such that when the case was wrapped around, the edges held onto each other. The lips were then spot-welded at regular 2" intervals. The lip and divots from the spot-welds can be seen in the bottom of Figure 42 below.

Figure 42: Top view of the stainless steel muffler case. Note the oblong shape and the lip at the bottom.

Unfortunately, the main case's shape did not closely match the shape of the end-chamber, as shown in Figure 43 and Figure 44 below. The case could not be plastically deformed into the correct shape due to its high yield strength; the material was unbelievably springy, in stark contrast to the mild steel used in the previous iteration. It could be held temporarily in shape by applying compression across its minor width using a large G-clamp, or multiple hose clamps and solid metal blocks.

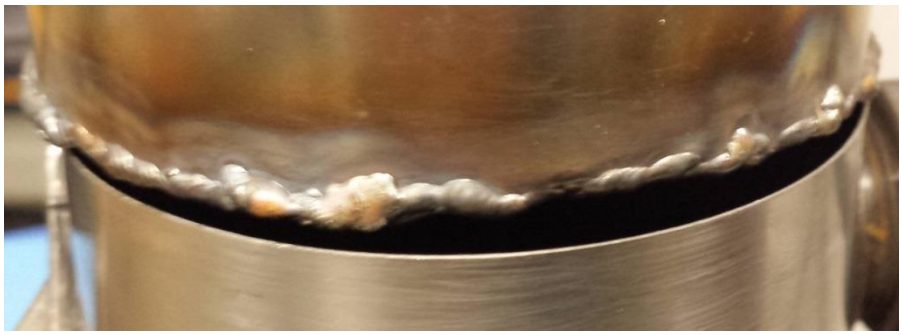

Figure 43: Lateral gap between the end chamber and main case.

Figure 44: Longitudinal gap between the end chamber and main case.

The lateral gap between the case and the end chamber was brought close enough together to weld using a combination of hose clamps and aluminium blocks, as shown on the right in Figure 45. The longitudinal gap was reduced by grinding back the weld bead on the end chamber. This is generally inadvisable as it can weaken the weld, however in this case it did not cause any issues. The resulting welds were still large and messy, due to the multiple beads required to fill the remaining gaps, and due to the thin material being difficult to weld in general.

Figure 45: The end chamber tacked to the main case. Left: Close-up. Right: View showing hose clamp jigs.

The endcap was fabricated by wrapping a strip of the 0.5mm stainless steel sheet around the main case, essentially using the endcap end of the muffler as its jig. The strip is raised above the edge of the case to avoid them becoming welded together, as shown below in Figure 46. Also shown in Figure 46 is a long steel bar and small piece of scrap sheet metal which are used to hold up the endcap bulkhead, as shown in Figure 47.

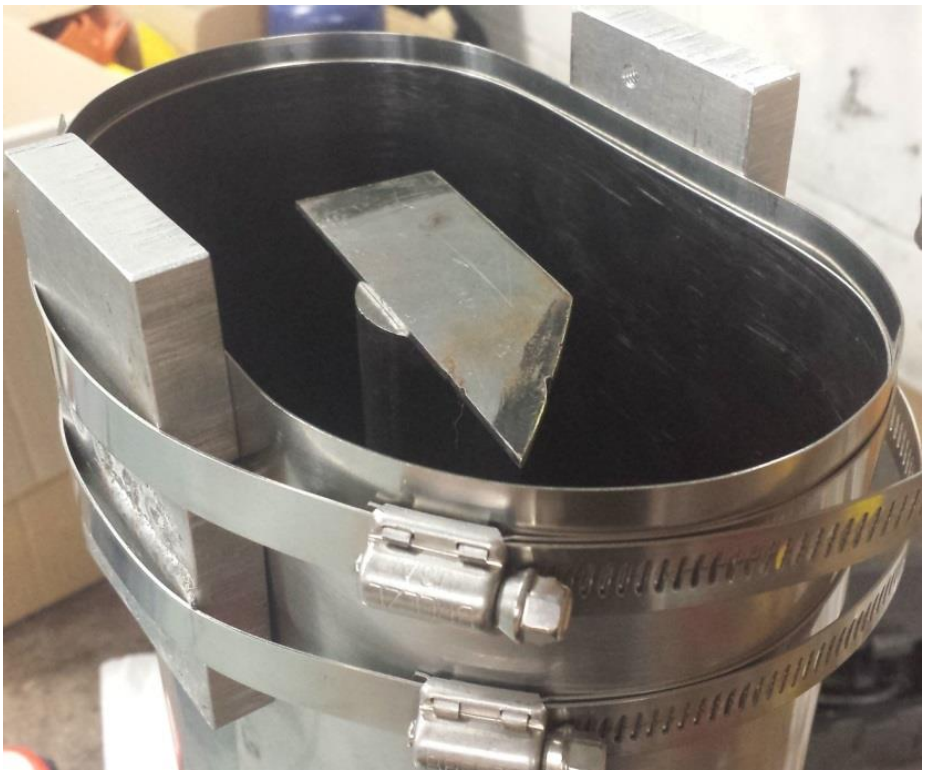

Figure 46: Endcap strip jigged to muffler case, and endcap bulkhead stand balanced in center.

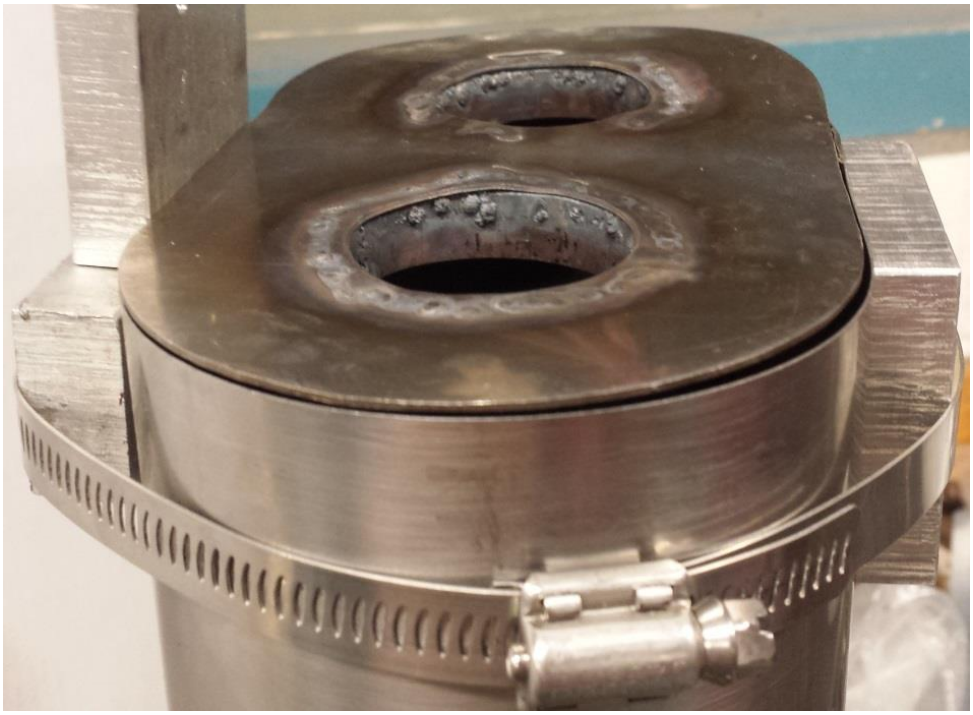

Figure 47: Endcap bulkhead resting on its stand, in line with the edge of the muffler case.

Figure 48 below shows the endcap fully welded and with rivet holes, but prior to the inlet and outlet tubes being attached. The high surface hardness of the stainless steel alloy made it incredibly difficult to drill the rivet holes straight. Both the centre punch and the drill bit tended to skid along the surface rather than deform or cut the material.

Figure 48: Welded and drilled stainless steel endcap. Note the rivet holes are not in line due to difficulties with the center punch and drill combined with the surface hardness of the steel alloy.

The stainless steel muffler prior to packing and the fitting of the inlet and outlet tube is shown in Figure 49. This photo shows a twist in the muffler case which could have been caused by the misalignment of the case when it was spot-welded, or by thermal warp when it was welded to the end-chamber.

Figure 49: Stainless steel muffler assembled and standing on its end chamber. Note the significant longitudinal twist. This is likely caused by the welds, or a lack of constraining jigs during welding.

The stainless steel muffler was successfully finished and weighed 2286g without glass, with approximately 1510g of fibreglass for a total nominal weight of 3796g, 1079g less than the mild steel muffler, which is a 22.13% mass reduction. The absorptive section is 450mm long, 50mm shorter than the mild steel version, with an absorptive volume of 5192cm^3. The finished stainless steel muffler is shown in use below in Figure 50.

Figure 50: The stainless steel muffler installed on M20-C at FS Sydney 2020.

2.6 Outlet geometries and noise testing

The Formula SAE-A rules (SAE, 2019) dictate that the noise test will be conducted with the microphone/noise meter 0.5m from the exhaust outlet, at a 45° angle to the centre axis of the outlet. This technically defines a continuous ring of possible noise test locations, though any section of this ring is excluded if the noise meter's line-of-sight to the exhaust outlet is obstructed. If the exhaust outlet is level or near-level with the ground, then the noise meter is held in the horizontal plane with the outlet, thus defining only two points in space rather than a continuous ring. If the vehicle has multiple exhaust outlets, then a noise test is conducted for each outlet and the loudest result is used. In the Formula Student (European) rules, the noise meter is held 0.5m from the outlet, in the horizontal plane of the outlet, in a direction 45° to the projection of the outlet's axis onto that horizontal plane. Thus, the location of the noise meter does not change in a European competition whether the outlet is parallel with the ground, or pointing upwards; the location only depends on the projected direction of the outlet in the horizontal plane. Therefore, in a European competition, pointing the exhaust outlet upwards is beneficial since it means the exhaust stream is directed further away from the noise meter.

The noise test is conducted with the engine at idle, and at a specified "speed" RPM which varies depending on the engine used. M19/20-C idles at 2000 RPM, and the speed test is conducted at 5500 RPM. The noise limits are 103dB at idle and 110dB at speed, in the C-weighted scale.

Figure 51: Outlet tips for testing. From top left: Sheathed, 90°, 1 inch, 1 inch twin, 1.5 inch, 1 inch quad.

Throughout the year, multiple concepts for ways to reduce measured noise levels by altering outlet geometry were devised. The six outlets shown above in Figure 51 were manufactured in order to test three basic concepts. The pie cut 90° outlet is to test the difference between pointing the exhaust behind the car, upwards, or to the side. The 2- and 4-outlet tips are to test if splitting the exhaust gases spreads out the noise over a larger area and thus reduces noise in front of any individual outlet. Unfortunately, the quad-tip was not tested due to interference with the undertray rear diffuser. The straight 1.5 inch and 1 inch tips are for control/comparison purposes. The sheathed outlet is a concept which mimics a noise-reduction technique seen on many civil turbojet engines. The extra annular channel around the outlet may reduce the transverse fluid velocity gradient, which in turn could reduce turbulence between the outlet and the atmosphere and thus reduce noise caused by turbulence. The concept is visualised in Figure 52.

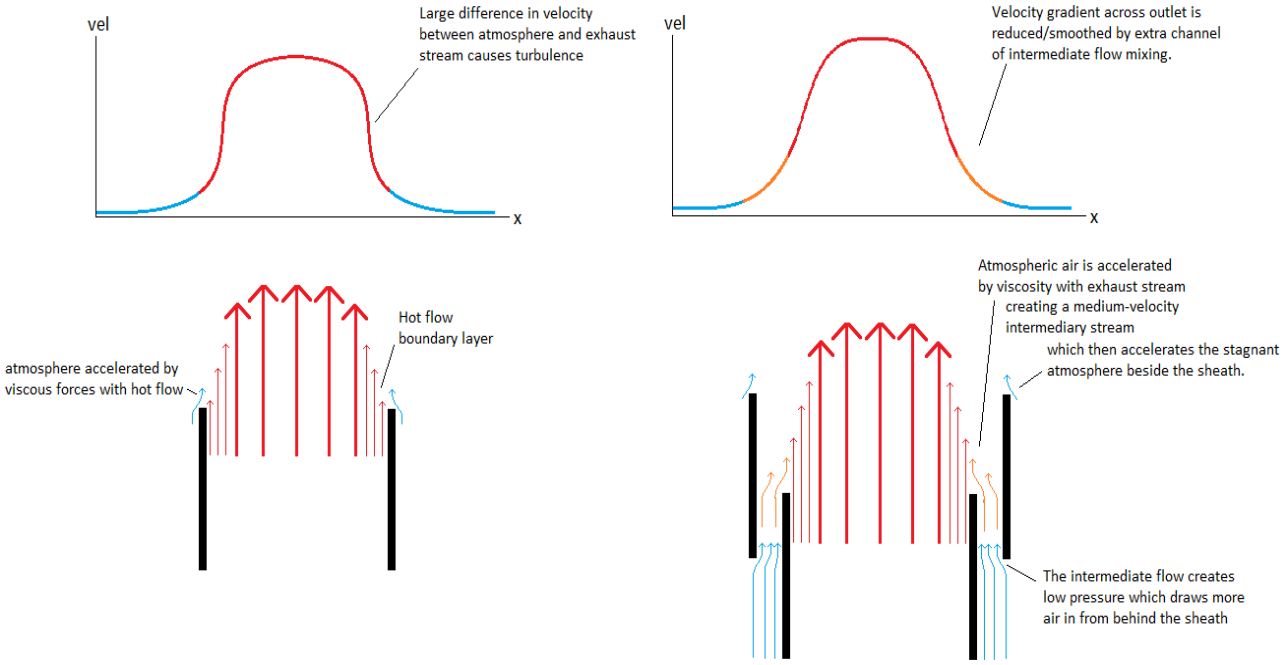

Figure 52: Illustrated and annotated explanation of logic behind the sheathed outlet. The sheath essentially may create a "bypass" air stream like in a turbojet engine, which reduces the severity of turbulent mixing.

Figure 53: Left: sheathed outlet before assembly. Right: Rolls-Royce turbojet exhaust pattern (boe747, 2010)

Additionally, testing was also done on outlet direction and placement. It was theorised from anecdotal experience that the car's rear wing endplates amplify engine and exhaust noise behind the car, like a soundshell. A simple 2D Java-based simulation (Falstad) is shown in Figure 54 to visualise this. The muffler was originally designed with an outlet facing backwards, approximately in the location of the red box on the left of Figure 54 below. By having the outlet point to the side of the car, the possible testing space is moved from the red and green lines to the green and blue lines shown on the left of Figure 54. This area to the side of the vehicle was found to be quieter both in the simulation and in practice, as presented in Table 2 below.

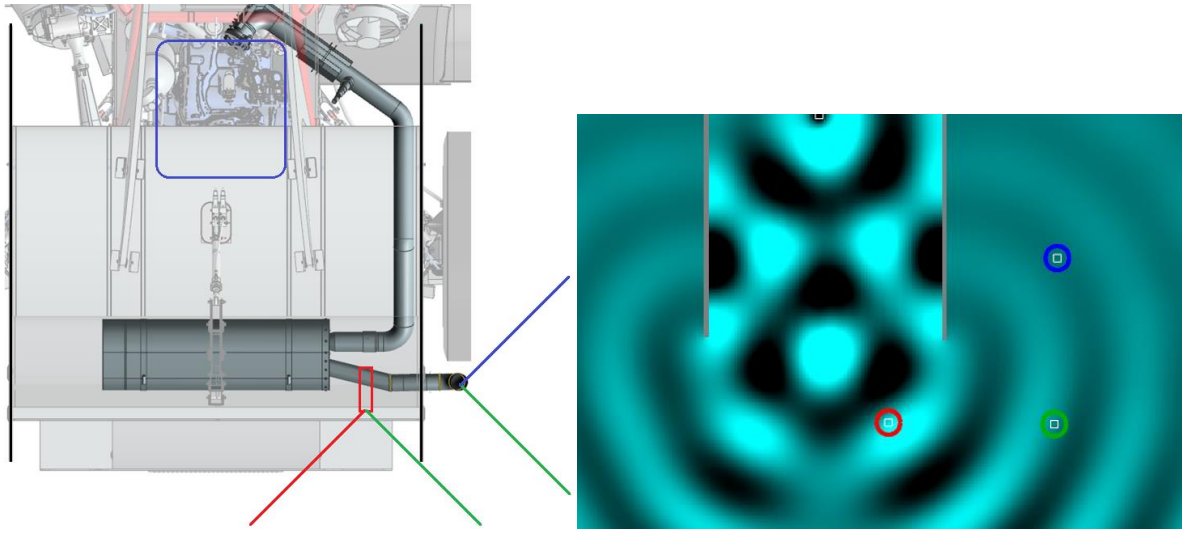

Figure 54: Left: Top view of rear of M20-C with bounds of noise testing space shown in red, green and blue lines. Right: Falstad Ripple (Falstad) simulation of noise level at the red, green and blue zones. Non-dimensional wave amplitudes are 248.93, 77.34, and 22.08, respectively.

Another concept tested was a "cross" of lockwire/safety wire across the outlet. This technique was used by some other teams at FSAE-A 2018. An example is shown below in Figure 55.

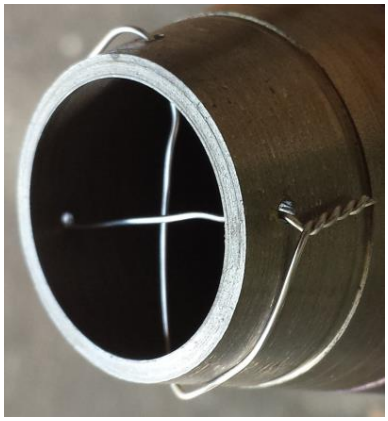

Figure 55: Lockwire/safety wire "cross" installed on an exhaust outlet.

Tables 1 and 2 below show a summary of findings from noise tests conducted during the project. The stainless steel muffler with no tip was 1dB above the limit at speed when tested at Monash University, however it passed the noise test at competition without the need for an attached outlet tip. This is likely due to differences in the testing venue; the competition test site is much more open and less prone to echoes than the space used at Monash University.

Table 1: Double-pass muffler noise results.

Muffler	Idle Noise Level (dB)	Speed Noise Level (dB)
Mild steel – 500mm absorptive length, no tip (38.1mm outlet)	100.2	108.5
Stainless steel – 450mm absorptive length, no tip	102.2	111

(38.1mm outlet)		

Table 2: Difference in noise levels resulting from tested conditions/geometries.

Change Tested	Idle Noise Delta (dB)	Speed Noise Delta (dB)
Measuring outside rear wing endplate, “green” area in fig. x.	-1.47	-3.63
Measuring outside rear wing endplate, “blue” area in fig. x.	-1.22	-5.58
Outlet safety wire cross (figure 55).	-0.15	-0.1
Reducing outlet size from 1.5 to 1 inch.	-1.45	-0.3
Splitting 1.5 inch outlet to two 1 inch outlets.	-4.6	-3.6
Adding sheath to 1.5 inch outlet, fig. x.	-0.75	-0.1
Delta between single and twin 1 inch outlets.	-2.55	-1.25

From the testing, it was concluded that:

- 450mm was just the right length of absorptive section, allowing the vehicle to pass the noise test with minimal unnecessary mass.
- The muffler’s outlet should be directed to the side of the car, and in a direction that causes the test to be conducted as far forward as possible. This is the most significant factor in measured noise level for the car.
- Reducing outlet size is a simple way to reduce noise level, but is not greatly effective.
- Splitting the exhaust into two outlets is a more effective way of reducing noise level than reducing the outlet size.
- A cross of safety wire has negligible impact on noise level.
- The sheathed outlet has negligible impact on noise level.

Additionally, the frequency spectrum of M19-C’s exhaust noise was measured and is presented below in Figure 56 and Figure 57.

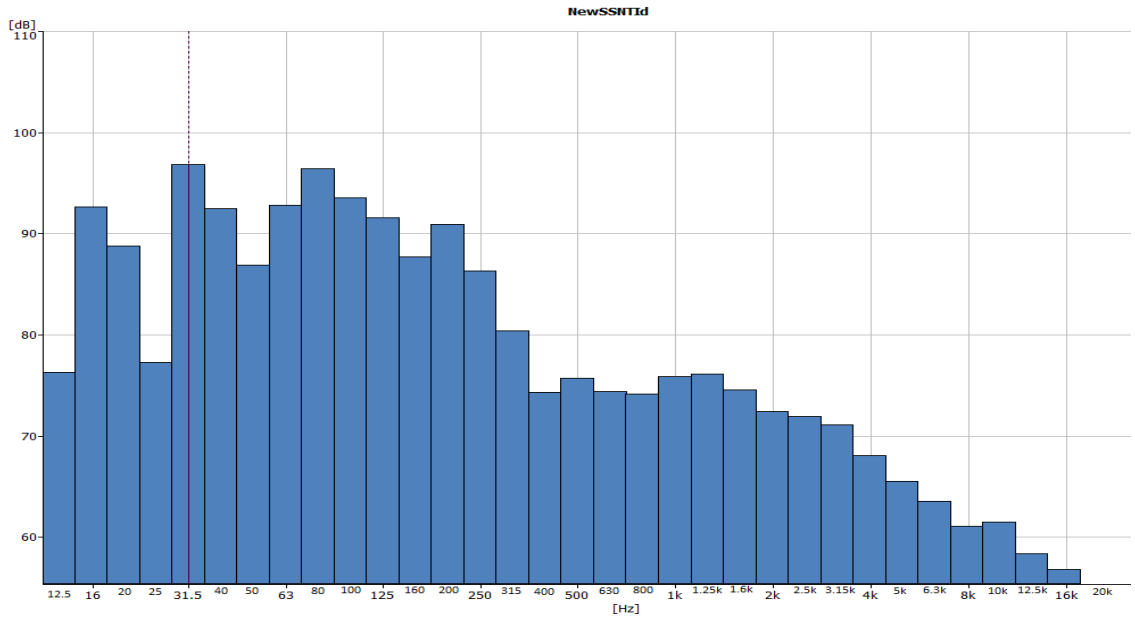

Figure 56: M19-C's frequency spectrum while idling at 2000 RPM. Note spikes at 16, 31.5 and 80 Hz.

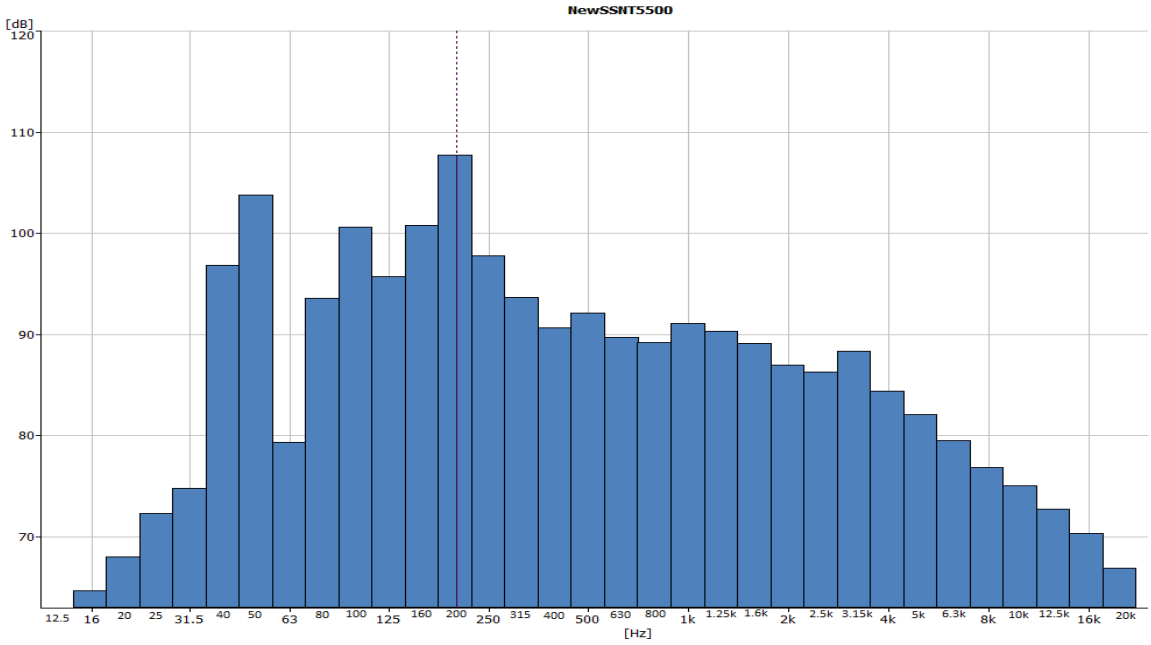

Figure 57: M19-C's frequency spectrum at 5500 RPM. Note spikes at 50, 100 and 200 Hz.

Since the vehicle most often fails the noise test at speed, a noise attenuating device which targets specific frequencies would be best tuned for 50, 100 or 200 Hz, as these are the three major peaks in the frequency spectrum at speed. The speed of sound in the exhaust gas, at a temperature of 500 C, is estimated to be about 520 m/s, though this would vary as temperature varies throughout the exhaust system. At that speed, the three major wavelengths during a speed noise test are 10.38m, 5.191m and 2.596m. As an example, a quarter-wave resonator would thus need to be approximately 649mm long to have a significant effect on the vehicle's noise level, though the exact length would need to be determined by physical tuning. This would be feasible, as this length is approximately the total length of the muffler including the outlet. A resonator side-branch which runs parallel to the muffler was designed but its manufacture and testing was cancelled due to the COVID-19 pandemic.

2.7 Fatigue, Cracks, and Failures

Cracks and other material failures were prevalent throughout the project. The exhaust system undergoes thermal cycles with temperature differences of 200-500K. It also experiences the strongest vibration of any system on the vehicle. Figure 58 below is a small montage of some of the various cracks which appeared and were repaired during the project. Every crack formed at the edge of a weld seam. Welds are considered a point of weakness in fatigue/cyclic loading, though this can be remedied by post-weld heat treatment. Such heat treatment was not used, as simply having spare parts to use in case of failures is a more cost-efficient option for this low-budget project.

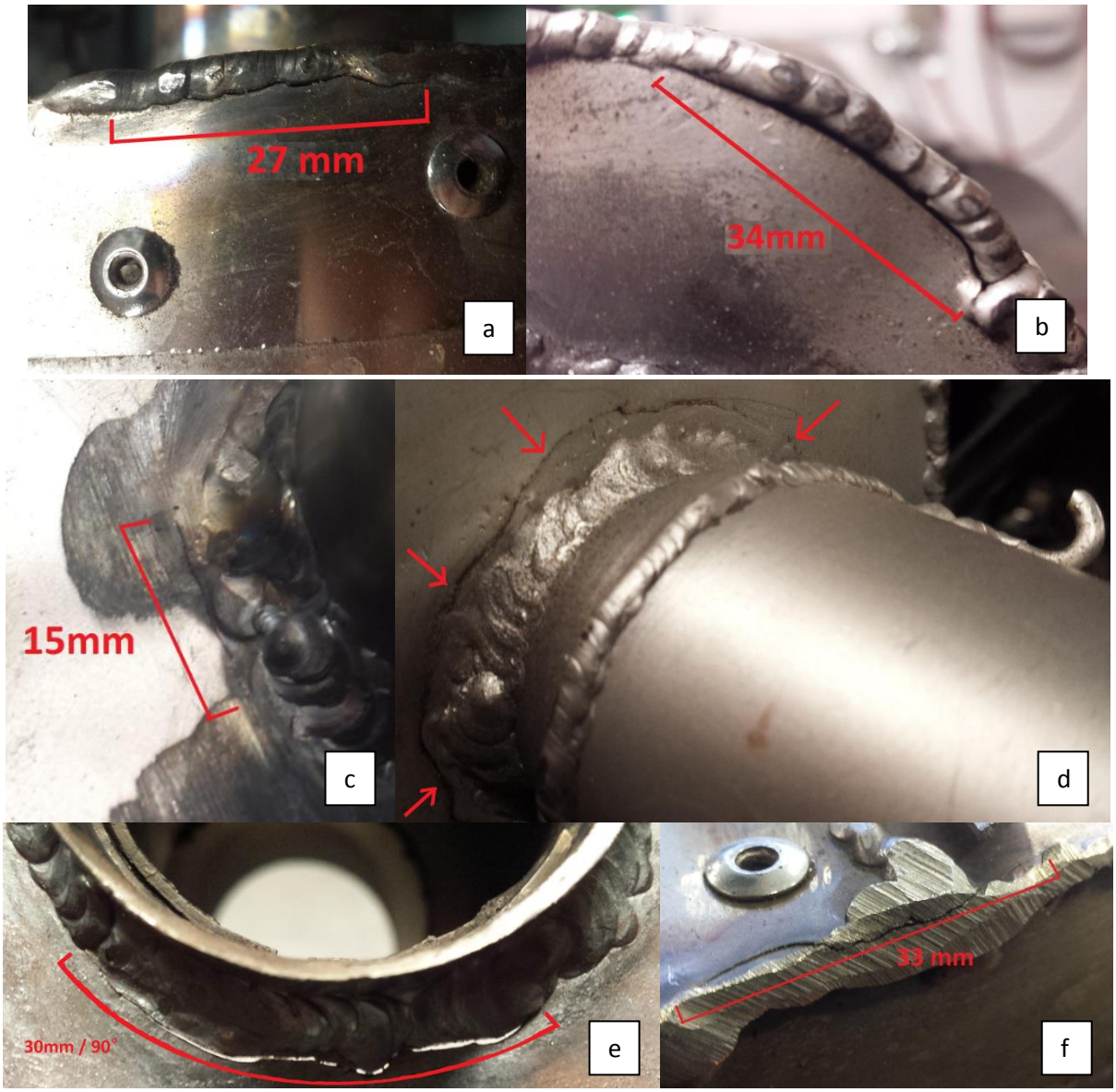

Figure 58: Various sizable cracks formed at welds. (a): Stainless steel endcap strip to bulkhead. (b): Mild steel endcap strip to bulkhead. (c): Mild steel endcap to outlet tube. (d): Mild steel inlet reducer to endcap. (e): Same crack as d, shown from inside. (f): Stainless steel endcap strip to bulkhead.

The most major muffler failure during the project was one of the reflector plates in the mild steel muffler coming loose. Figure 59 below shows the end chamber autopsy/inspection.

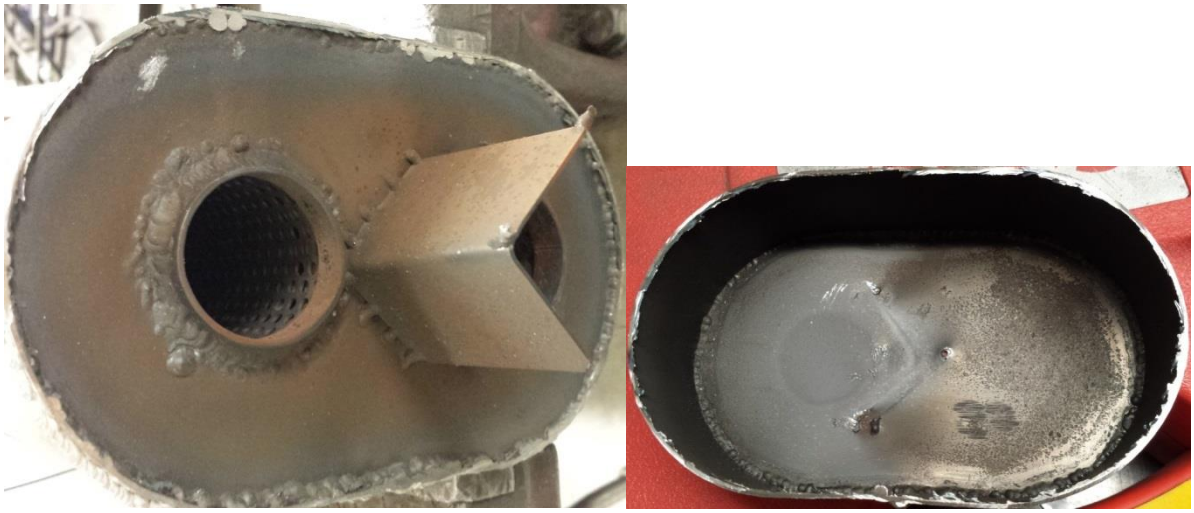

Figure 59: Left: Mild steel muffler inner bulkhead after removal of end chamber case. Note there is only one attached reflector plate. Right: The removed end chamber case.

The loose reflector plate is shown below in Figure 60. The reflector plates are tacked to both the inner and outer bulkheads of the end chamber. Since the inner bulkhead is in direct contact with the fibreglass packing, and the outer bulkhead is open to the atmosphere, it is theorised that the two plates have a significantly different temperature during operation, and this temperature difference caused strain in the reflector plate due to differential thermal expansion. The failure was repaired simply by cleaning the parts and welding the plate back on, but this time the reflector plates were only welded to the inner bulkhead, and a 1mm gap was left between the top of the plates and the outer bulkhead, to allow clearance for thermal expansion and contraction. Neither this issue nor any similar issue arose again.

Figure 60: The failed reflector plate. Note the formation of highly reflective iron nitride, or "mill scale". This layer has high surface hardness and cannot be scratched with a file.

During the back-pressure testing conducted as part of section 2.1 above, the copper pressure tap tube was damaged and fell off of the car. The flared end of the tube which forms a seal near the pressure tap boss in the exhaust manifold failed first, which caused the plastic portion of the pressure tap tube to fall down onto the exhaust manifold and subsequently melt. It is likely that the

copper flare underwent rapid fatigue, as it was mounted in a fashion which loaded the flare with the weight of the entire tube in a cantilever fashion. This was remedied on M19-C by mounting the pressure sensor underneath the manifold, so the fastener is loaded in tension rather than bending.

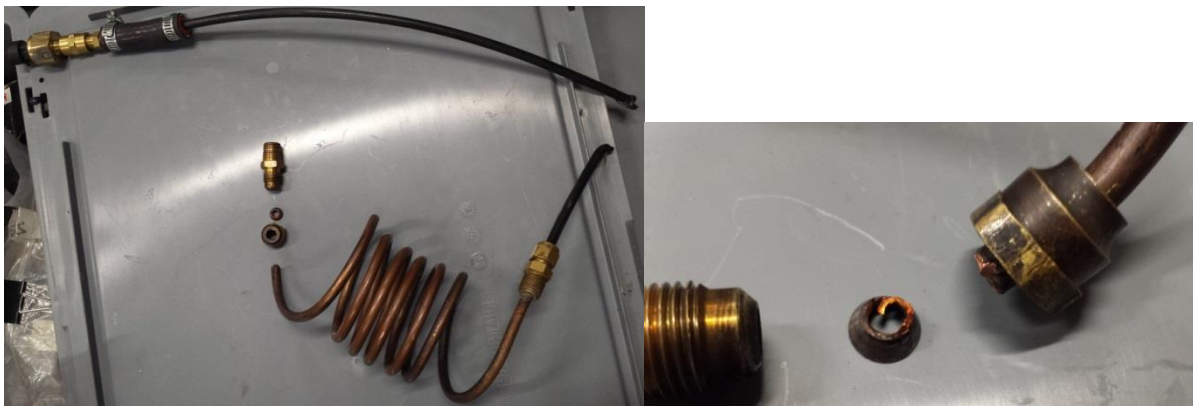

Figure 61: Left: All pieces of the failed pressure tap system. Right: Close-up of the torn copper flare.

2.8 Fibreglass Loss Study

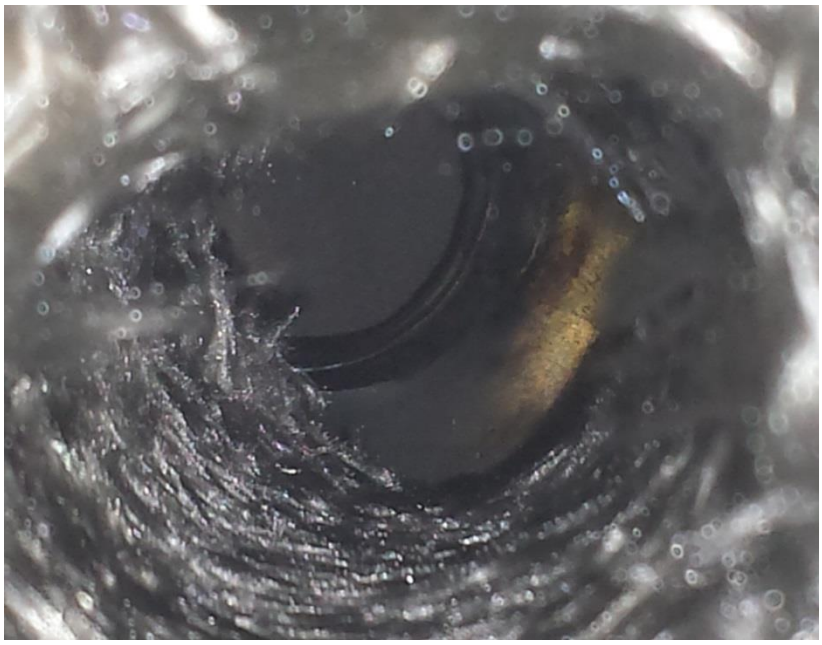

Figure 62: The hollow space formed at the closed end of the stainless steel muffler's absorptive section, viewed through the cavity from the removed perforated tube.

Inspection of the stainless steel muffler after 290km of testing revealed a hollow cavity of missing fibreglass at the closed end of the absorptive section, as shown above in Figure 62. In addition, there were also regularly spaced holes in the packing material between the two perforated tubes. The holes were spaced apart from each other by 20mm and ran the length of the absorptive section of the muffler, though they reduced in size further into the muffler and were largest near the inlet/outlet end cap. These holes are shown in Figure 63, prior to removal from the muffler.

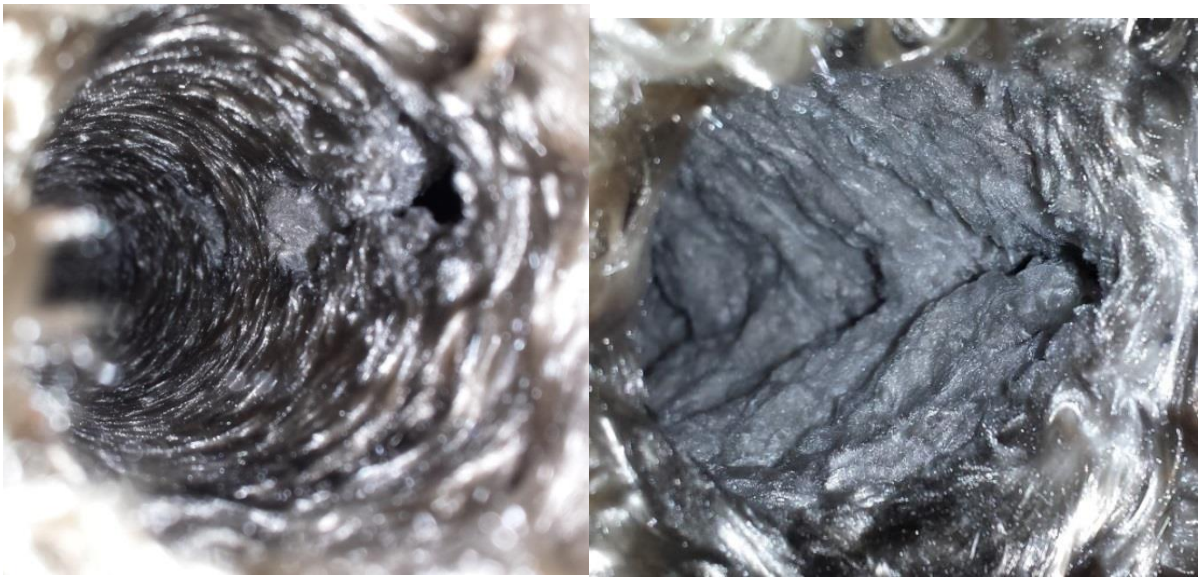

Figure 63: Regularly-spaced holes in the fiberglass packing material between the two perforated tubes. Left: Inlet side. Right: Outlet side.

The fibreglass was removed from the muffler, revealing a cone-shaped pattern to the holes. The smaller side of the holes were up against the inlet perforated tube and they enlarge through the space between the tubes until reaching the outlet side perforated tube. A cross section of one of these cavities is shown in Figure 64. It appears that a portion of the gas flow was "taking a shortcut" through the fibreglass, instead of following the route through the end chamber and all 900mm of perforated tubing. This would likely be causing increased noise levels, as a component of the sound waves can travel directly from the muffler's inlet to its outlet through the cavities with minimal noise attenuation from the packing material.

Figure 64: A cut-away of one of the holes formed between the perforated tubes.

Upon removal of all of the fibreglass, the large hollow cavity from Figure 62 above becomes clearer. It is slanted, with more glass having gone missing from the inlet side of the muffler. A comparison of the removed fibreglass placed alongside the muffler is shown below in Figure 65.

Figure 65: All the fiberglass absorptive material removed from the stainless steel muffler after 290km of testing. The fiberglass mass is lined up with the muffler case. Note the large missing mass of fiberglass to the left, on the closed end of the muffler.

In addition to the hollow cavities of missing glass, some of the fibreglass had formed into hard cyst-like formations. These can be seen above in Figure 65 and also below in Figure 66 after having been picked off of the fibreglass mass. All of the fibreglass was in the form of continuous strands when the muffler was packed. However, these growths consisted of a powdery mass of miniscule glass fibres which almost seemed sintered together into hard, organically-shaped tumour-like formations. They formed only near the wall/case of the muffler, and only on the top side. Potentially their formation is caused partially by rapid cooling, as their proximity to the muffler case would cause them to lose heat to the atmosphere faster than the fibreglass closer to the centre of the muffler.

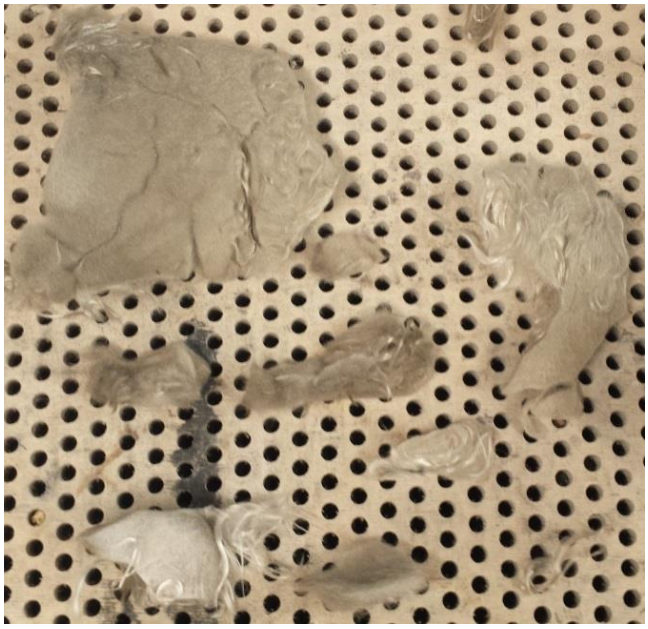

Figure 66: The hard powdery fiberglass "growths", removed from the muffler.

During routine repacking, the mild steel muffler was also found to form a hollow cavity at the closed end of its absorptive section, more so on the inlet side, as shown below in Figure 67. This can also be seen in the pattern of cured high-temperature paint on the muffler's external surface; the paint that was used turns a darker grey colour upon reaching a specified "bake on"/curing temperature. The paint was not cured before the muffler was installed on the car as it was believed that the paint would cure from the heat of the exhaust gas. However, after a few testing sessions it became apparent that the only sections of the case to become hot enough for the paint to cure were sections which were in direct contact with exhaust gas due to missing fibreglass. Since the loss of fibreglass follows the same pattern in both versions of this muffler and thus demonstrates repeatability, it is likely due to a flaw in the muffler's design. It is possible that such issues could be avoided by advanced flow analysis of future muffler designs, such as by utilising computerised fluid dynamics (CFD). However, these techniques require a significant time investment in order to be conducted accurately, and were thus considered outside the scope of this project. A much more resource-efficient strategy is to simply repack the muffler more often, as necessary.

Figure 67: Top: fiberglass removed from the mild steel muffler, showing a missing mass in the bottom right. Bottom: The corresponding pattern of cured paint, in the same location as the hollow cavity.

To test whether the conical holes from Figure 64 could be mitigated, two solid stainless steel sheets were tack-welded to the perforated tubes and the muffler was repacked with the shields facing each other, as shown in Figure 68. These would prevent the exhaust gas from flowing directly between the tubes. For gas to transfer between the tubes without going through the end chamber, it would need to travel around these sheets and thus through a longer path of fibreglass packing, which would provide greater resistance to gas flow and thus hopefully a greater portion of gas would be routed through the end chamber.

Figure 68: Repacking the stainless steel muffler with steel "shields" welded to perforated tubes.

Unfortunately, these solid sheet shields were ineffective. After approximately 50km of testing, the muffler's end cap was removed and the fibreglass was inspected again. Holes in the fibreglass had still begun to form, at the edges of the solid shields, as shown in Figure 69. A solution to this issue could be designed. However, any additional device/geometry added to the muffler would increase mass, and finding a working solution would require a significant time investment. It was decided that the most efficient use of resources, given the scope of this project, would be to simply accept that fibreglass will inevitably be lost from the muffler over time, and to repack it as necessary.

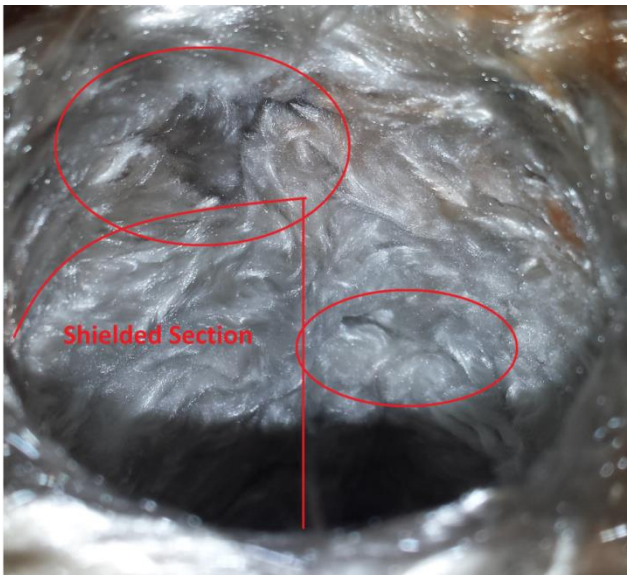

Figure 69: Holes forming in the fiberglass around the shielded section of the perforated tube.

The rate at which fibreglass is lost from the muffler was recorded over a number of weeks for both the mild and stainless steel mufflers. The mufflers were weighed after each testing session, and it is assumed that any reduction in mass is due to the expulsion of glass fibres. The findings are shown below in Figure 70. This fibreglass loss study unfortunately does not include many data points due to the mufflers needing to be repacked or repaired after only a few testing sessions. It appears that the mild steel muffler experienced logarithmic loss of its fibreglass, while the stainless steel muffler lost its glass seemingly linearly. The cause of this difference is unknown. The best-fit rate of fibreglass loss for the stainless steel muffler is 0.095% per kilometre, or 10% every 105.3 kilometres.

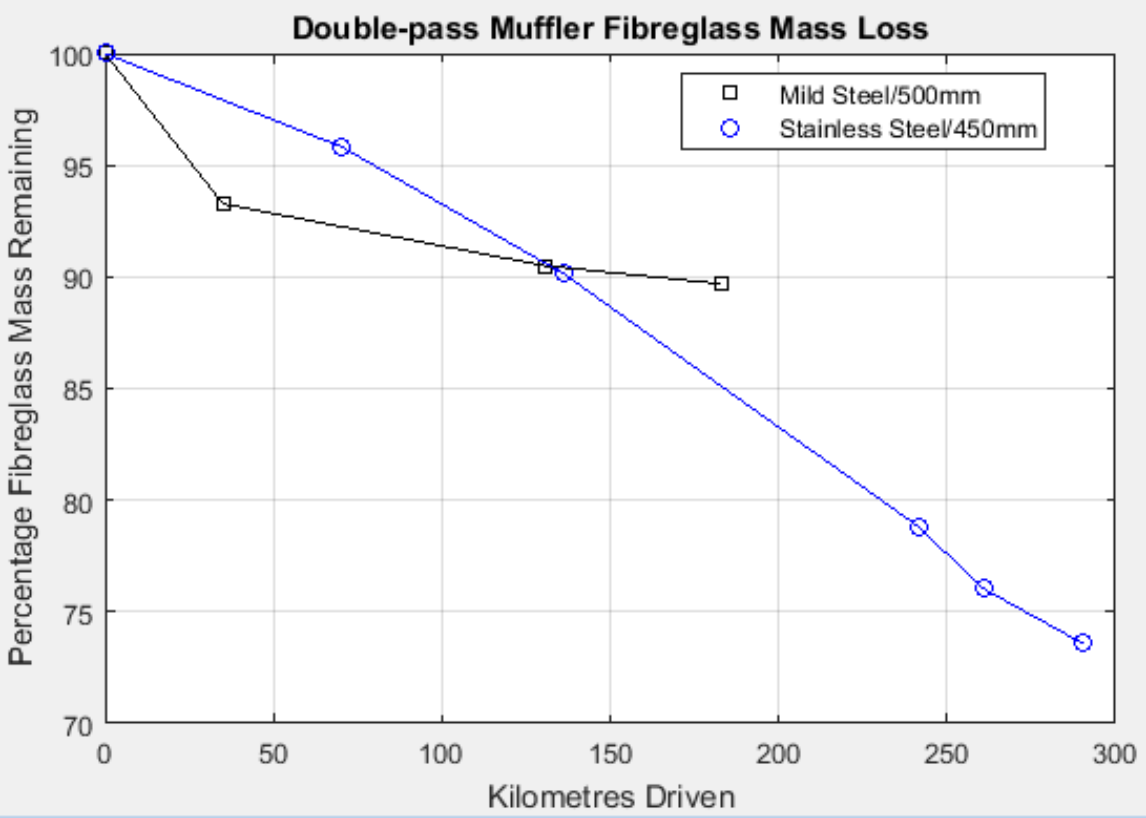

Figure 70: Fibreglass lost vs. kilometers driven. The mild steel muffler's mass seemed to almost reach a plateau before it required repacking. The stainless steel muffler, conversely, continued to lose mass at a steady rate.

2.9 Unfinished Projects

There were five additional significant avenues of development for the exhaust system which were investigated, but unfortunately were not pursued. They are as described below.

2.9.1 Stamped Endcaps

Muffler endcaps were manufactured throughout the project using a flat plate as a face/ bulkhead, and a long strip of metal bent/rolled around its circumference and then welded at the edges, perpendicular to the face plate. It was theorised that a stamp die could be developed which will allow endcaps to be made faster, and without any welds, thus reducing failure points. Unfortunately, only four prototype endcaps were made, and none were of usable quality. The stainless steel muffler's endcap was thus welded in the traditional way to save time. Figure 71, Figure 72 and Figure 73 show the stamp die, and Figure 74 and Figure 75 show the resulting stamped endcap which was not able to be used.

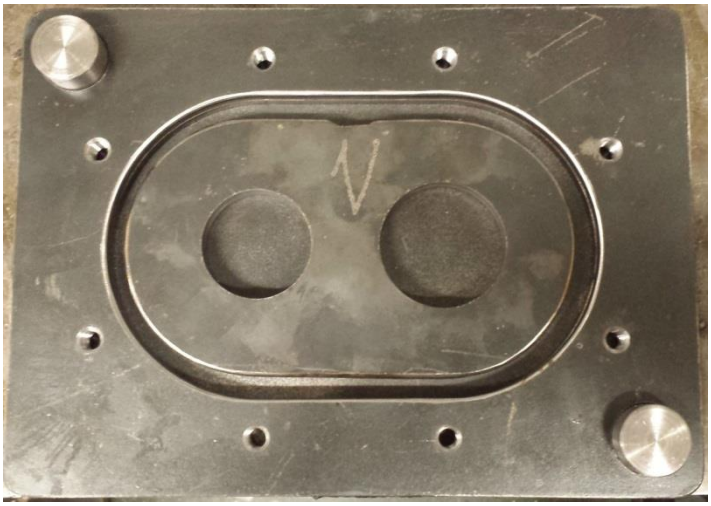

Figure 71: The female endcap die stamp.

Figure 72: The male endcap die stamp.

Figure 73: The combined die, showing how the male ring will fit into the female, pushing the flat endcap stencil into the cavity and forming an endcap shape.

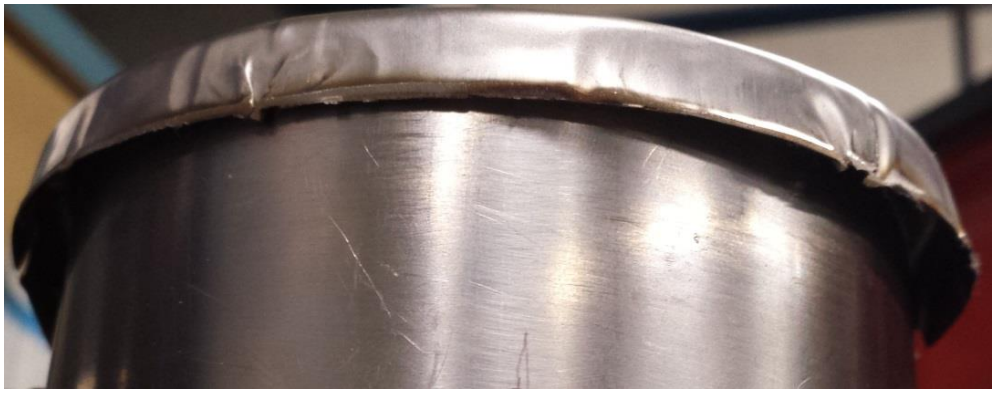

Figure 74: The highest quality stamped endcap out of the four attempts, placed over the stainless steel muffler main case to demonstrate the large gap and rippling which made the endcap unusable.

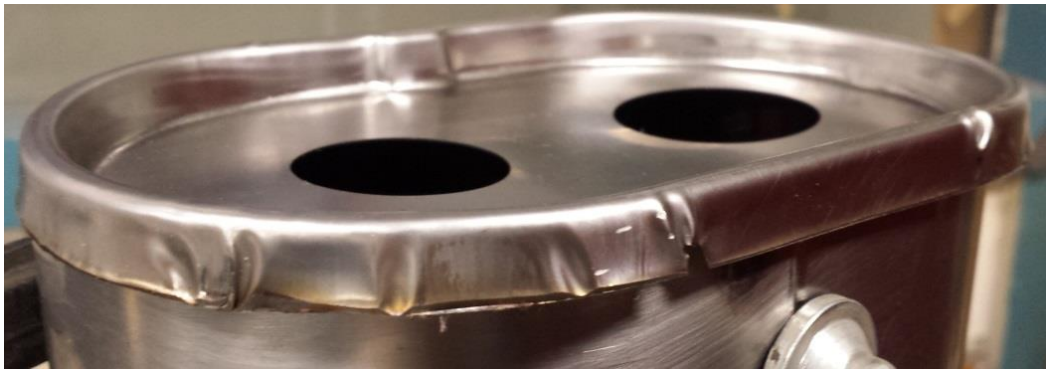

Figure 75: The same endcap as from figure 70, shown from above. The endcap is almost usable; a second iteration of the die would only need to solve the rippling problem.

2.9.2 Acoustic Test Bench

Throughout MM's history, muffler geometry has been designed based on trial-and-error. Like the outlet noise testing in section 2.6, testing new noise-reducing geometries requires manufacturing the device(s) to a fully functional quality and then testing them on the car, which requires organising testing time with the rest of the team. An “acoustic test bench” would allow the exhaust designer to rapid-prototype noise-reducing devices and test them without them needing to be installed on the car, which would help improve the rate of development of noise-reduction technology throughout future years.

The most rigorous type of acoustic test bench would test transmission loss, which measures a device’s noise absorption and reflection abilities independently of the surrounding system (Bowden, 2016). To do so would require a setup with multiple independent microphones logging pressure data at high frequency, in a highly controlled environment.

A simpler form of acoustic test is to test for insertion loss, which simply involves attaching a speaker to one end of the device to be tested and measuring the noise on the other side of the device, and then taking a control measurement by attaching the speaker to a tube of the same length of the device (Herrin, D. W.). The insertion loss is the noise loss associated with “inserting” the device into the system, replacing the tube. This type of test provides less comprehensive data on the device but is much more within MMS’s capabilities in terms of facilities and budget.

A spare speaker was acquired and its frequency spectrum was measured, as shown in Figure 76. This graph shows the speaker's ability to produce each frequency of sound. Figure 57 shows that MMS' car produces most noise below 4kHz, with spikes at 50, 100 and 200 Hz. However, this speaker's ability to produce sound diminishes below 250Hz. Hence, this 70mm speaker would likely not have been sufficient for MMS's purposes; a larger speaker capable of producing lower frequencies would have been more useful. Regardless, the project was abandoned before completion due to the COVID-19 outbreak. This is most unfortunate, as an acoustic test bench would potentially be the greatest source of development in the design techniques for MMS's future exhaust systems.

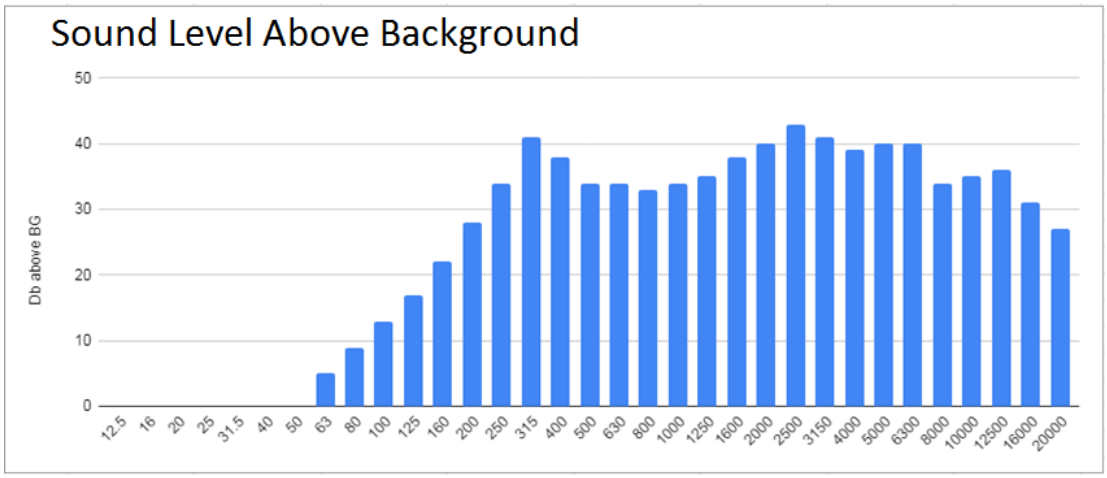

Figure 76: Frequency capabilities of prospective speaker for insertion loss test bench.

2.9.3 Newer Stainless Steel Muffler Manufacture

Prior to the COVID-19 outbreak, MMS was planning on participating in Formula Student competitions in Europe. These European competitions would have a much higher expectation for build quality and parts' finish. Thus, it was decided that it was in the team's best interest to produce another stainless steel muffler, but this time with more purpose-made jigs to avoid the thermal warping issues encountered by the first one. A "ribcage" style jig was designed, a new fabrication order was devised which reduced the amount of welds necessary by half, and parts were cut out and ready to be welded. A new stainless steel case was also spot welded in the same style. The jig bulkheads/ribs are shown in Figure 77 prior to cutting. Unfortunately, the team ceased activity due to COVID-19 before the jigs could be welded together or any other further progress made.

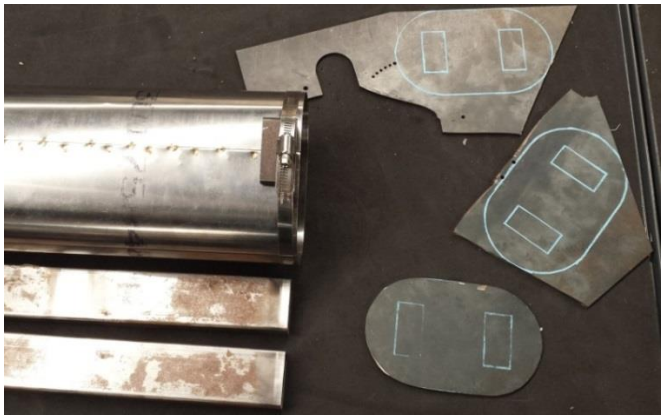

Figure 77: The new case, jig bulkheads and jig spines prior to fabrication.

2.9.4 Dynamometer Back-pressure Testing

The exhaust system on MMS's dynamometer is attached to an extraction unit which creates suction on the attached exhaust. This causes back-pressure applied to the dynamometer engine to be very different and likely lower than the back-pressure on the car, and the dyno engine thus likely overestimates the M20-C's engine power. In order to tune the dynamometer's exhaust pressure to match the car's, a guillotine-style valve was acquired from SGV Exhaust Brakes in New South Wales, and it was fitted to the dynamometer exhaust system. The valve is an exhaust brake usually used on trucks to increase back-pressure as a way of slowing down heavy vehicles without wearing down brake pads. The dynamometer exhaust brake could also be used to test for and acquire a much more accurate back-pressure/engine power relationship than the on-track testing from section 2.1. The brake is fully installed on the dynamometer but unfortunately the testing was cancelled due to the COVID-19 outbreak. This particular avenue of development was planned to be the main source of this project's improvement to the team's points simulator, as set out in the objectives of the project. Fortunately, the on-track back-pressure testing from section 2.1 still provides some insight into the relationship between competition points and back-pressure, but testing it on the dynamometer would have been much more rigorous and likely would have provided more accurate results. Photos from the installation of the exhaust brake are shown below in Figures 78 through 82.

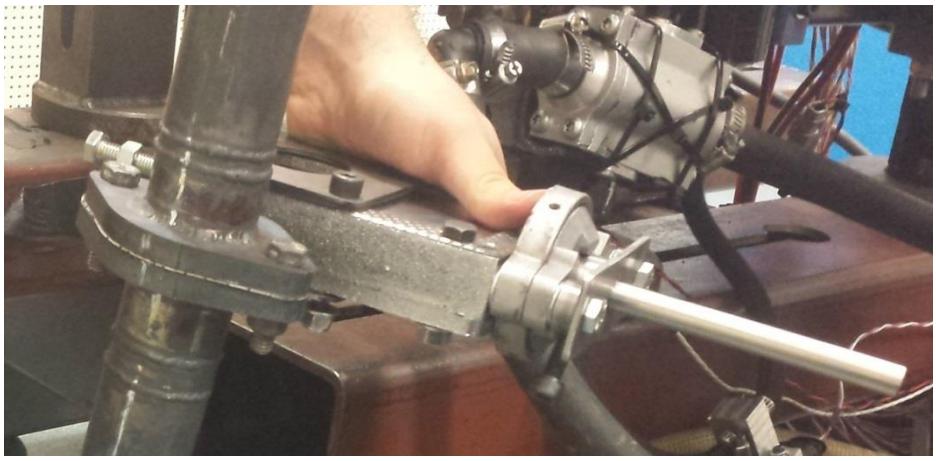

Figure 78: The exhaust brake prior to installation.

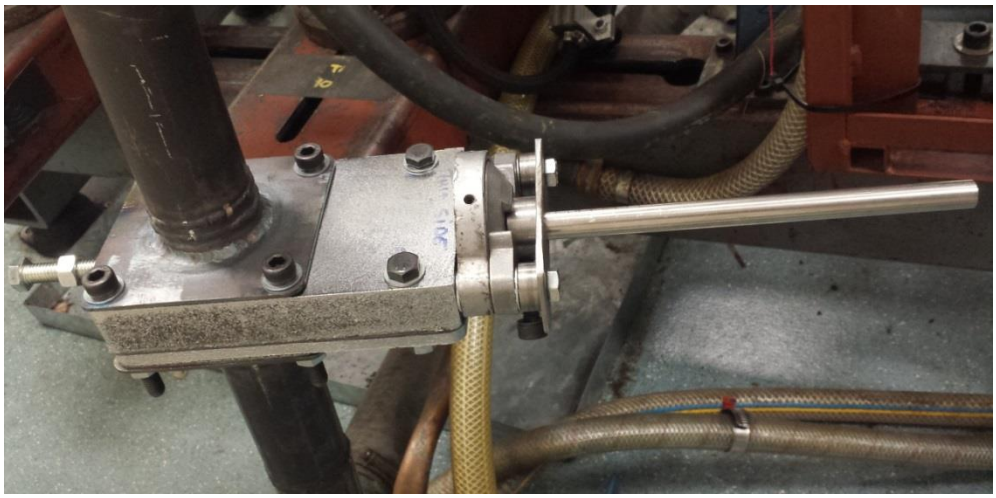

Figure 79: The exhaust brake installed on the dynamometer, replacing the existing two-bolt flange.

Figure 80: The dynamometer's exhaust system, including new brake.

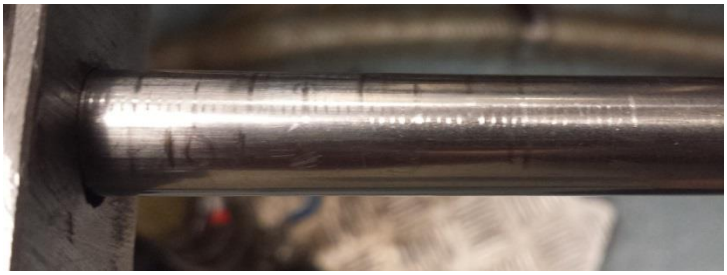

Figure 81: Marks made in the rod of the guillotine valve every millimeter which allow the valve to be opened to specific positions.

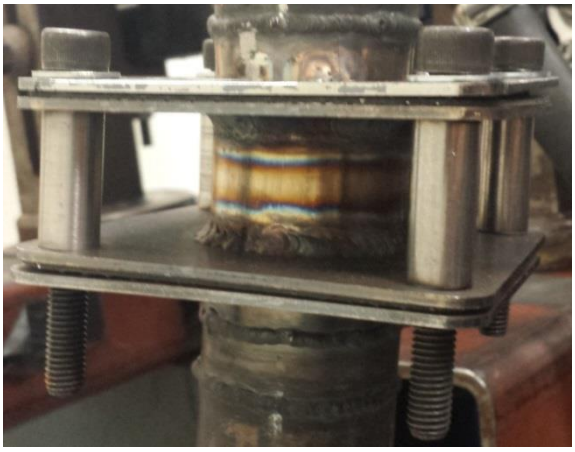

Figure 82: A straight tube spacer which can replace the exhaust brake in case it is uninstalled.

2.9.5 Adjustable Helmholtz Resonator

A Helmholtz resonator is essentially a closed tube that branches off of the exhaust tube. Sound waves split at the intersection, and the portion that travels up the resonator will reflect off the closed end and re-join the exhaust flow back at the intersection. Wavelengths of noise which are 4 times the length of the resonator will arrive back at the intersection half a wavelength out of phase, and will thus destructively interfere. Such a device could be effective at reducing total noise level if its length is tuned to match the wavelengths most prevalent in the KTM 690's frequency spectrum. A Helmholtz resonator was manufactured which could fit in the 1.5 inch outlet slip join of the muffler, and can be seen below in Figure 83. The resonator's closed end was formed by a plug which could be moved in or out by turning a long threaded rod, thus changing the resonator's target frequency. Unfortunately, the device was never tested due to the COVID-19 outbreak.

Figure 83: Left: View through the resonator's open section. Right: Photo of the resonator, showing the branched-off section and the threaded rod which allows for tuning.

3. SYSTEM DESIGN

Through the testing, experimentation, and development shown above, the following final design for M20-C's exhaust system has been reached, including CAD screenshots in Figures 84 through 87.

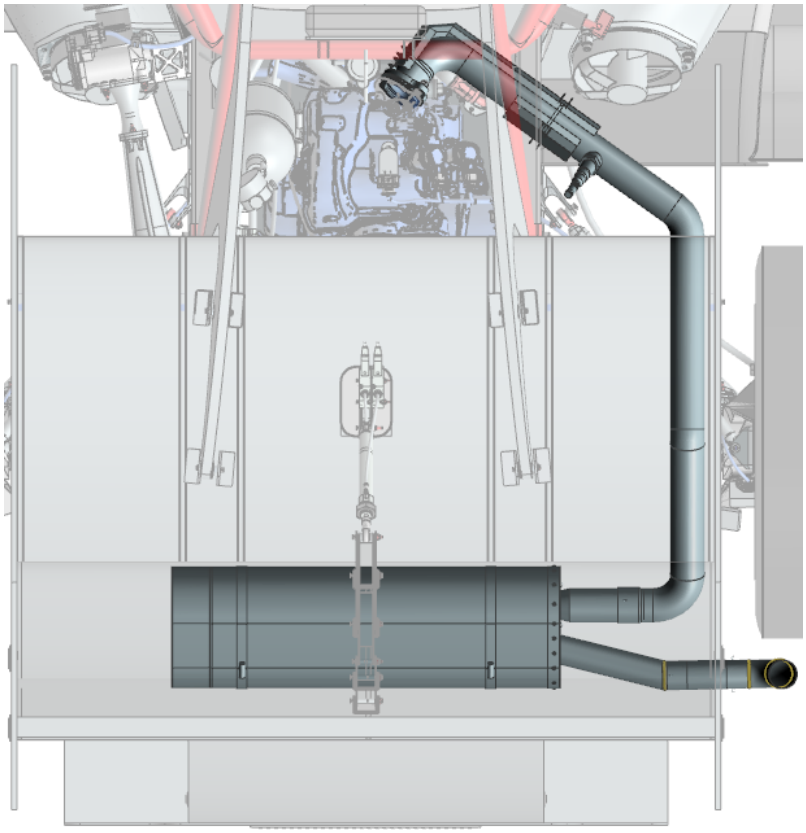

Figure 84: Top view of exhaust system CAD.

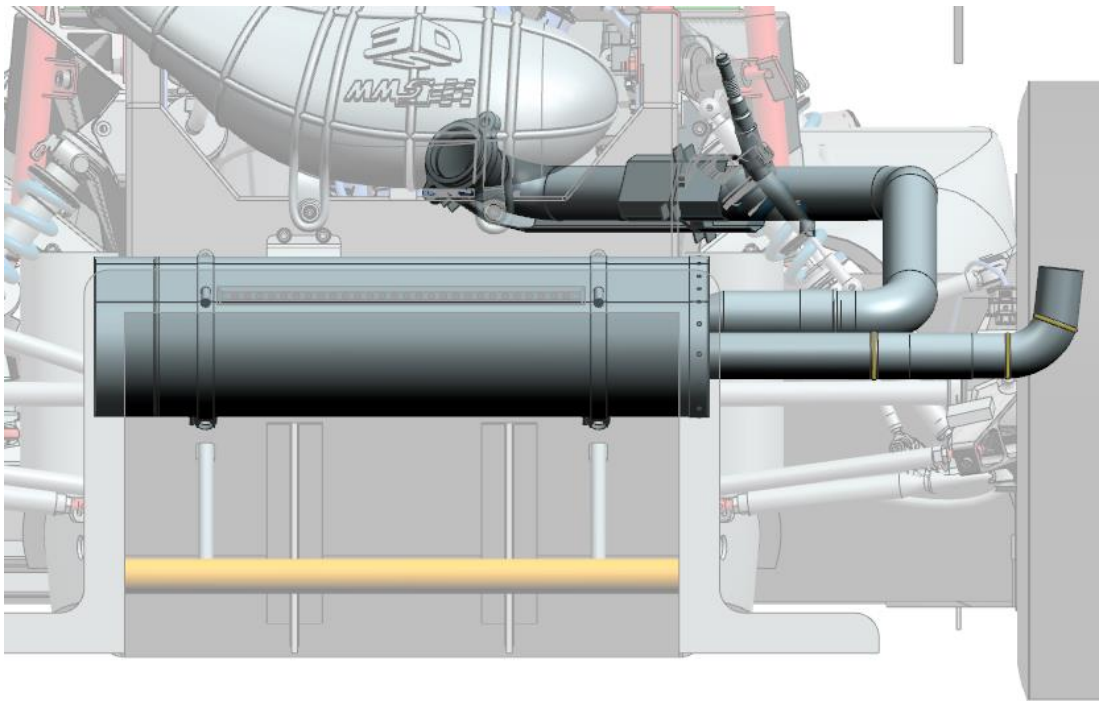

Figure 85: Rear view of exhaust system CAD.

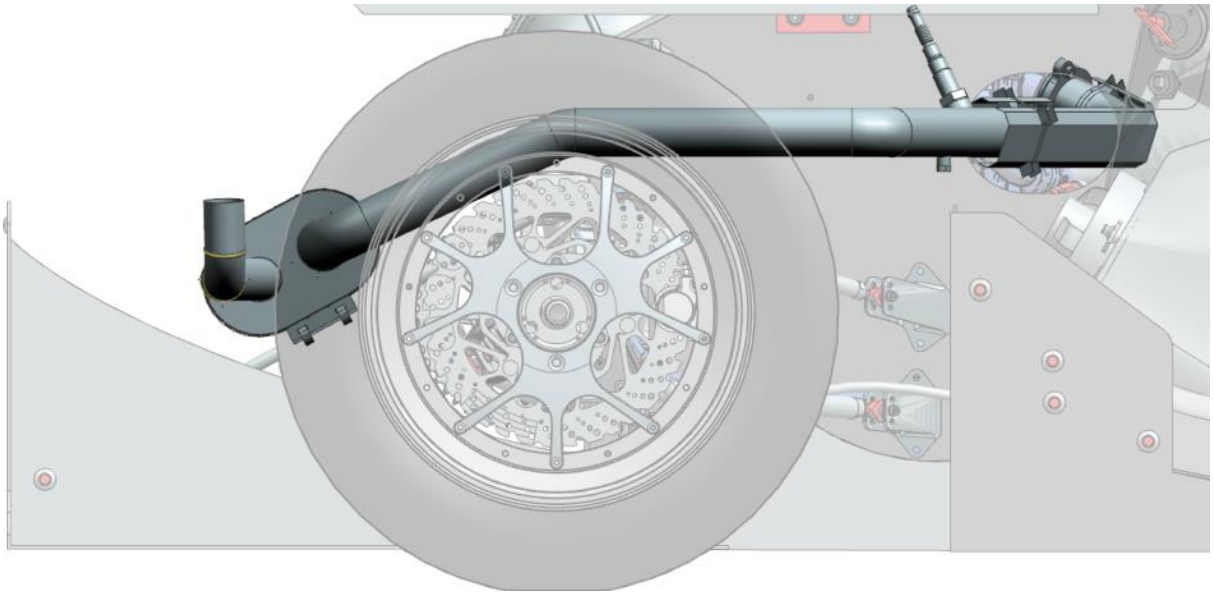

Figure 86: Side view of exhaust system CAD.

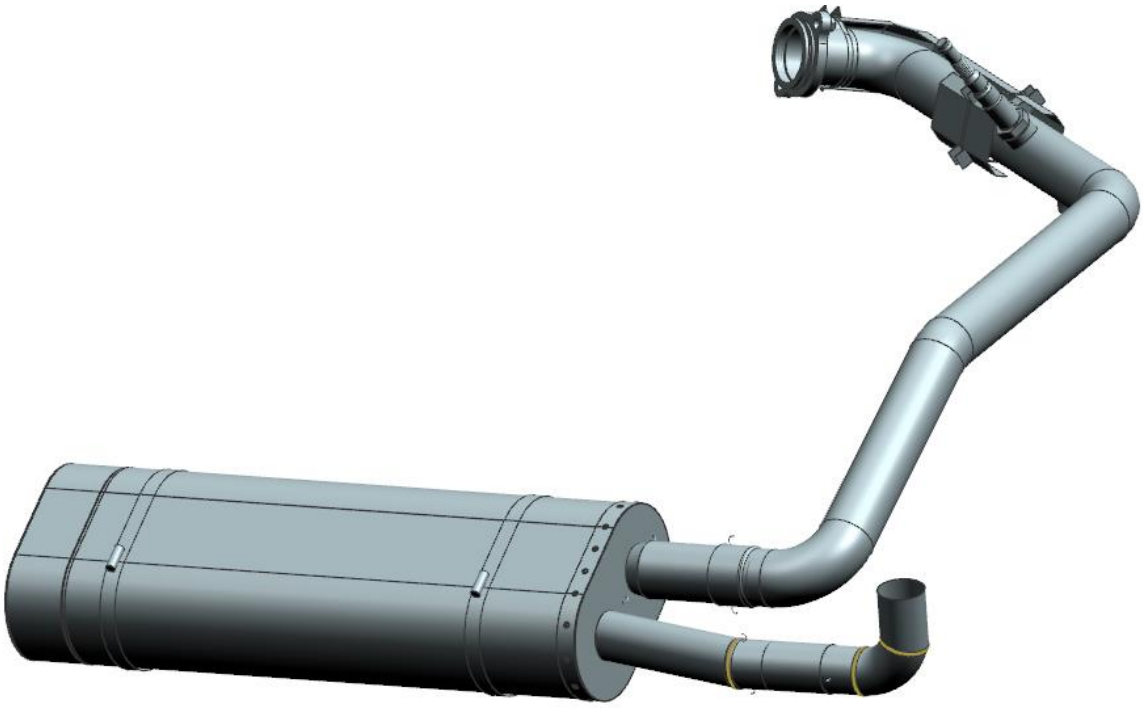

Figure 87: Angled view of exhaust system CAD.

The exhaust manifold consists of 1.75 inch (44.45mm) outer diameter stainless steel tube, which is TIG-welded with an argon purge system. The size matches the header of the KTM Duke-R 690 engine which is already chosen for the vehicle. Stainless steel has greater corrosion resistance than mild or carbon steels, which is important in the hostile environment of the exhaust. It is also much cheaper and easier to weld than titanium, which is another popular high-performance exhaust material. Unfortunately, titanium is not available as a material due to financial limitations. The manifold connects to the engine via a 2-bolt flange, which matches the studs provided on the engine. It is also fitted with threaded bosses for an oxygen (lambda) sensor, and a pressure sensor.

The exhaust is routed through a hole in the side of the car's monocoque chassis, then backwards over the rear right suspension to the muffler. The muffler uses a space above the rear diffuser of the undertray. The outlet of the muffler then goes to the right side of the car, also going further rearwards in order to avoid interference with the rear right tyre. This route is shown in Figures 84 through 87 above. It is the most direct route to the rear of the car, which is the safest place to exhaust the gases, while avoiding proximity to heat-sensitive components.

Heat is managed in three ways:

1. The entire manifold is ceramic coated, which greatly reduces heat transfer over the whole tube, especially from radiation.
2. A triple-layer heat shield is mounted to the bend near the engine, the hottest section of the exhaust. The heat shield also extends far enough to shield the chassis as the exhaust passes through the hole. The inner layer of the shield is 0.3mm-thick stainless steel which can resist high temperatures. The outer layer is 0.2mm-thick aluminium, which maintains a low temperature via its highly dissipative properties. A central layer of ceramic fibre felt insulates the two metallic layers, which are both dimpled. The shield is mounted via stainless steel cable ties onto prong mounts welded to the manifold, which create a 10mm space between the tube and the heat shield, ensuring effectiveness.
3. The chassis near the hole is covered by an adhesive-backed reflective and insulating sheet, to minimise heat transfer into the heat-sensitive chassis in proximity to the exhaust.

The muffler is also made from stainless steel, and is a double-pass design which increases perforated tube length and absorptive volume in a compact space. The gas is redirected into the second perforated tube via a hollow chamber rather than a bent tube/pipe as the expansion space reduces noise transfer. Two chevron-shaped reflector plates in this chamber block some noise from reaching the outlet and also create a channel which causes dispersion and destructive interference of sound waves. The muffler's internals and outlet are 1.5 inch in diameter, and there is a 1.75-1.5 inch reducer on the inlet of the muffler to facilitate this. The muffler has a removable, riveted end cap on one side to allow access for inspection and repacking. It connects to the manifold via a sprung slip joint, and is mounted with hose clamps to two round steel struts which bolt to the monocoque chassis.

The outlet of the muffler ends in a female slip joint, which facilitates the attachment of various outlet/tip designs. For competitions in which it provides an advantage (European and Sydney), an outlet which redirects the flow upwards can be used in case the vehicle does not initially pass the noise test, though this should not be necessary. For FSAE-A, where directing the exhaust outlet upward also changes the defined noise test location, a twin-outlet tip is available for contingency instead.

With this exhaust system installed, M19-C won 1st place overall at FSAE-A and FS Sydney 2020, and won 1st at FSAE-A Design Event 2019 (SAE-A, 2019) (FS-Sydney, 2020). M20-C, a minor revision of M19-C, is planned to be used by MMS as a driver training vehicle for the foreseeable future.

4. CONCLUSIONS

Through constant experimental development, this project has concluded with the following results, findings, and observations:

- A high-performance FS/FSAE exhaust system was successfully designed, passed the noise test and technical inspection of multiple competitions, and the vehicle won 1st place overall at FSAE-A and FS Sydney 2020, and won 1st at FSAE-A Design Event 2019.
- Information was gathered through testing and documentation of fabrication methods which will assist future MMS exhaust designers in creating higher-performance systems
    - Back-pressure testing conclusively found that the double-pass design is superior to a single-pass design with the same attenuation ability.
    - Noise testing of many exhaust configurations led to improvements in exhaust outlet placement and geometries; directed out from the side of the vehicle, and splitting the exhaust to multiple outlets.
    - An argon purge system is highly effective at improving weld quality in enclosed stainless steel welds. An open-top argon purge tank is not effective at improving weld quality in non-enclosing parts, though it does reduce oxidation somewhat.
    - To improve the service life of mufflers in the future, common failure points can be avoided by minimising and/or heat-treating welds, and avoiding over-constraining of parts.
- A rough relationship was found between exhaust back-pressure and competition points, being approximately 0.55 points per kPa of pressure.

Thus, all three major objectives of the project set out in the introduction have been achieved.

5. ACKNOWLEDGEMENTS

MMS' sponsors, such as Altair, MoTeC, CigWeld, Hare & Forbes, Wago, Laser3D, DCI Performance Products, Monash University Mechanical and Aerospace Engineering Department, and KTM.

All members of MMS for assisting the project indirectly, by maintaining the team's car, and helping during testing sessions.

Scott Wordley, Michael Crocco, and all of MMS' leadership and management, for running the team which made this project possible. Especially Scott Wordley, for supervising this project.

William Jenkin, exhaust designer from 2016, for general advice on the system's development.

Mason Lees, for helping with some of the welding, the development and testing of the endcap stamps/dies, and for spot-welding the stainless steel muffler case.

Sukith Wehella, for assistance such as weld fit-up and cleaning for some of the outlets/tips and the Helmholtz resonator, as well as some modifications to the final system design CAD.

Various businesses and suppliers, such as TRR Auto Parts, Best Mufflers, ECS Engines, International Karting Distributors, Bunning Warehouse, ENZED, RS Components, Bralco/Airport Metals, Hampdon, Silent Sport, Brüel & Kjær, and SGV Exhaust Brakes.

6. REFERENCES

Beranek, Leo L. "NOISE AND VIBRATION CONTROL", Institute of Noise Control, Revised edition 01/06/1998, ISBN 978-0962207204, page 370.

boe787, 26/03/2010, "*A quiet word about noise*", accessed 04/06/2020: https://boe787.wordpress.com/2010/03/26/a-quiet-word-about-noise/

Bowden, David R. 2016, "Development of a large experimental acoustic transmission loss test bench suitable for large marine diesel exhaust system components", accessed 04/06/2020: https://www.acoustics.asn.au/conference_proceedings/AASNZ2016/papers/p54.pdf

Falstad, Paul. "*Ripple Tank Version 1.3*", accessed 04/05/2020: https://www.falstad.com/ripple/

FS-Sydney: Powered by ARDC, 2020, accessed 04/05/2020: https://www.facebook.com/FSSydney2020/posts/2388892484549073

Herrin, D. W., Ph.D., P.E., University of Kentucky Department of Mechanical Engineering, "Measurement of Muffler Insertion and Transmission Loss", accessed 04/05/2020: http://web.engr.uky.edu/~dherrin/Bandung/15_Measurement_of_Mufflers_and_Silencers.pdf

Kimbrough, Bobby. 11/03/2020, "Understanding Muffler Design and Sound Absorption Strategies", Rod Authority, accessed 04/06/2020: https://www.rodauthority.com/tech-stories/exhaust/understanding-muffler-design-and-sound-absorption-strategies/

Monash Motorsport, 2020, "*Staging for brake test under smoky Sydney sky*", accessed 04/06/2020: https://www.facebook.com/photo/?fbid=2919686571385909&set=a.2919541481400418

Praveen, V. and Sethupathi, P., "Active Muffler for Single Cylinder Engine, Using Electronic Throttle Control for Formula Student Cars," SAE Technical Paper 2017-28-1935, 2017, doi:10.4271/2017-28-1935.

RCW Aerospace Specialist Welding Systems, "About Our Welding Chambers", accessed 04/06/2020: https://www.rcw-aerospace.com/AboutOurWeldingChambers.html

Society of Automotive Engineers Australasia, 2019, "2019 Formula SAE-A Results", accessed 04/06/2020: http://www.saea.com.au/2019_Results

Society of Automotive Engineers International, 2019, "Formula SAE Rules 2019", accessed 04/06/2020: https://www.fsaeonline.com/cdsweb/gen/DownloadDocument.aspx?DocumentID=64b861c2-980a-40fc-aa88-6a80c43a8540

7. APPENDICES

Appendix A: Additional/unused figures.

Muffler	Tip	Diametre (mm)	Configuration	Test speed	RPM	Leq(C)
MS double pass	None	38.1	inside endplate	Idle	2000	102
MS double pass	None	38.1	inside endplate	Speed	5500	111.7
MS double pass	None	38.1	outside endplate	Idle	2000	100.2
MS double pass	None	38.1	outside endplate	Speed	5500	108.5
MS double pass	1.5"	34.6	No Lockwire, outside endplate	Idle	2000	100.1
MS double pass	1.5"	34.6	No Lockwire, outside endplate	Speed	5500	107.3
MS double pass	1.5"	34.6	No Lockwire, inside endplate	Idle	2000	101.3
MS double pass	1.5"	34.6	No Lockwire, inside endplate	Speed	5500	111.4
MS double pass	1"	23.3	Lockwire, outside endplates	Idle	2000	98.2
MS double pass	1"	23.3	Lockwire, outside endplates	Speed	5500	107.1
MS double pass	1"	23.3	Lockwire, inside endplates	Idle	2000	100
MS double pass	1"	23.3	Lockwire, inside endplates	Speed	5500	110.8
MS double pass	1"	23.3	No Lockwire, inside endplates	Idle	2000	100.3
MS double pass	1"	23.3	No Lockwire, inside endplates	Speed	5500	111.3
MS double pass	1"	23.3	No Lockwire, outside endplates	Idle	2000	98.2
MS double pass	1"	23.3	No Lockwire, outside endplates	Speed	5500	106.8
MS double pass	Twin	22.4	inside endplate	Idle	2000	97.2
MS double pass	Twin	22.4	inside endplate	Speed	5500	108.8
MS double pass	Twin	22.4	outside endplate, rear	Idle	2000	96.2
MS double pass	Twin	22.4	outside endplate, rear	Speed	5500	106.8
MS double pass	Twin	22.4	outside endplate, front	Idle	2000	96
MS double pass	Twin	22.4	outside endplate, front	Speed	5500	104.5
MS double pass	Duel stream	34.6	inside endplate	Idle	2000	100.4
MS double pass	Duel stream	34.6	inside endplate	Speed	5500	111.4
MS double pass	Duel stream	34.6	outside endplate	Idle	2000	99.5
MS double pass	Duel stream	34.6	outside endplate	Speed	5500	107.1
MS double pass	Pointing sideways	34.6	Forward	Idle	2000	98.5
MS double pass	Pointing sideways	34.6	Forward	Speed	5500	105.2
MS double pass	Pointing sideways	34.6	Rear	Idle	2000	97.8
MS double pass	Pointing sideways	34.6	Rear	Speed	5500	106.8

Figure a: Full noise test results of outlet tip testing on the mild steel muffler.

Muffler	Tip	Diametre (mm)	Measurement location	Test speed	RPM	Leq(C)
New SS double	None	38.1	Behind and to side of car	Idle	2000	102.2
New SS double	None	38.1	Behind and to side of car	Speed	5700	110.2
New SS double	None	38.1	Behind and to side of car	Speed	5500	111
New SS double	None	38.1	Behind and to side of car	Speed	5500	112.1
New SS double	1" - with lockwire holes	23.3	Behind and to side of car	Idle	2000	100.6
New SS double	1" - with lockwire holes	23.3	Behind and to side of car	Speed	5500	110
New SS double	Twin - Cut down	22.4	Low outlet	Idle	2000	99.9
New SS double	Twin - Cut down	22.4	Low outlet	Speed	5500	110.2
New SS double	Twin - Cut down	22.4	High outlet, close to endplate	Idle	2000	98.6
New SS double	Twin - Cut down	22.4	High outlet, close to endplate	Speed	5500	108.7
New SS double	Twin - Cut down	22.4	High outlet, away from endplate	Idle	2000	97.3
New SS double	Twin - Cut down	22.4	High outlet, away from endplate	Speed	5500	106.1
New SS double	Twin - Cut down	22.4	High outlet, inside endplate	Speed	5500	112.5

Figure b: Full noise test results of testing the twin tip on the stainless steel muffler.

Figure c: Left: Small crack in a stainless steel muffler weld, main case to outer end bulkhead. Right: The same small crack after sanding the surface.

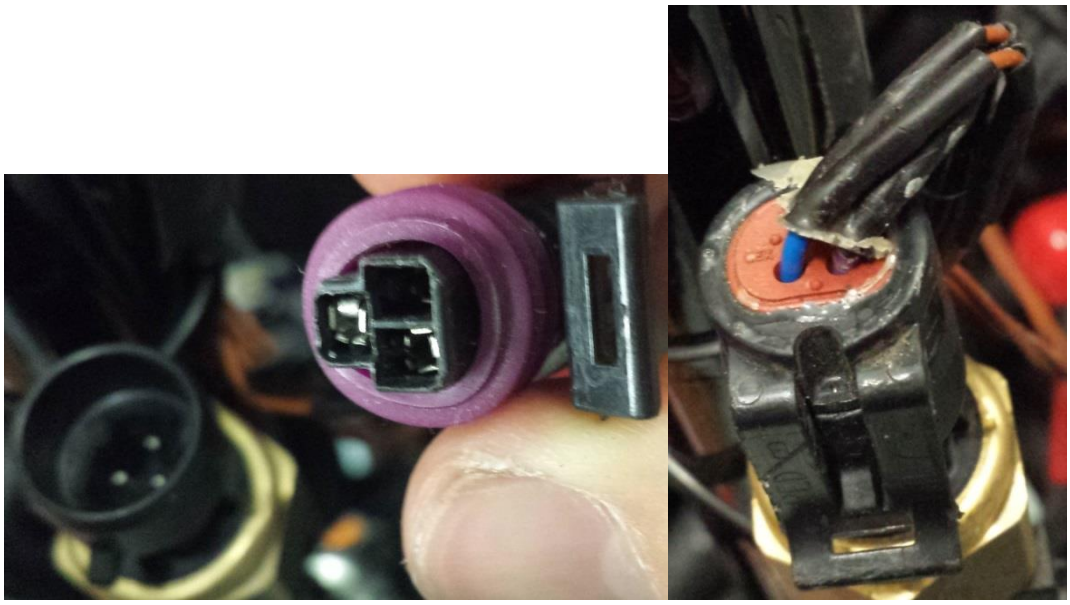

Figure d: Pull-out failure of pressure sensor connector due to operator error during uninstallation.

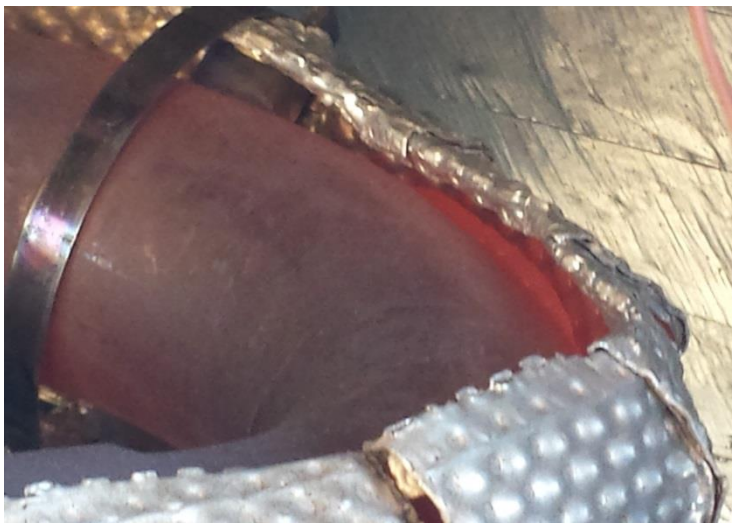

Figure e: Cherry-red glow of exhaust header from under the heat shield.

Figure f: Various parts used in the assembly of the exhaust, muffler and welding purge box.

Figure g: Mild steel muffler inner bulkhead being welded using aluminium blocks and clamps.

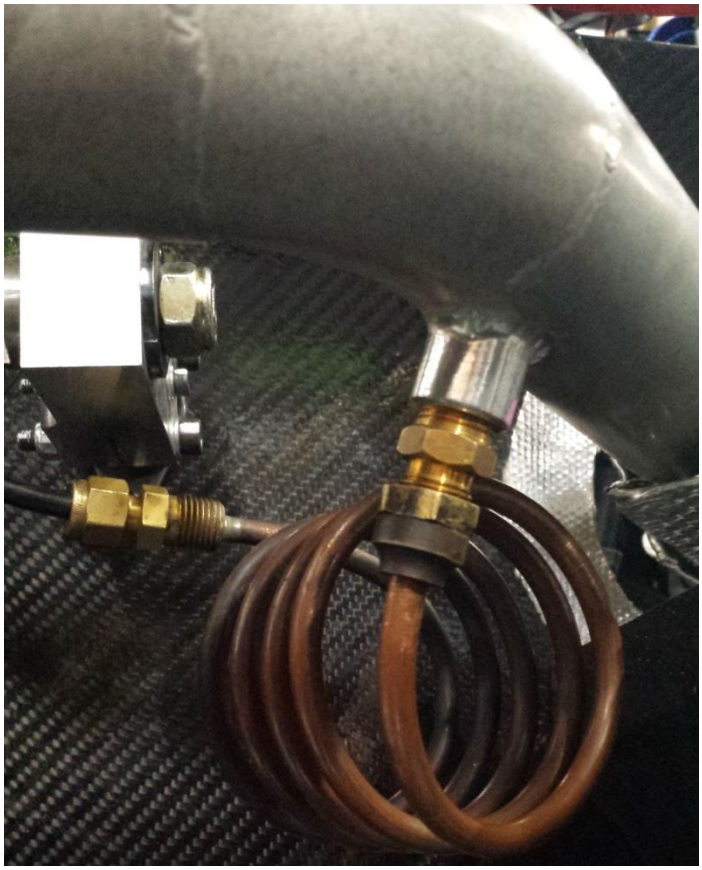

Figure h: The pressure sensor tap tube installed underneath the M19-C's exhaust manifold.

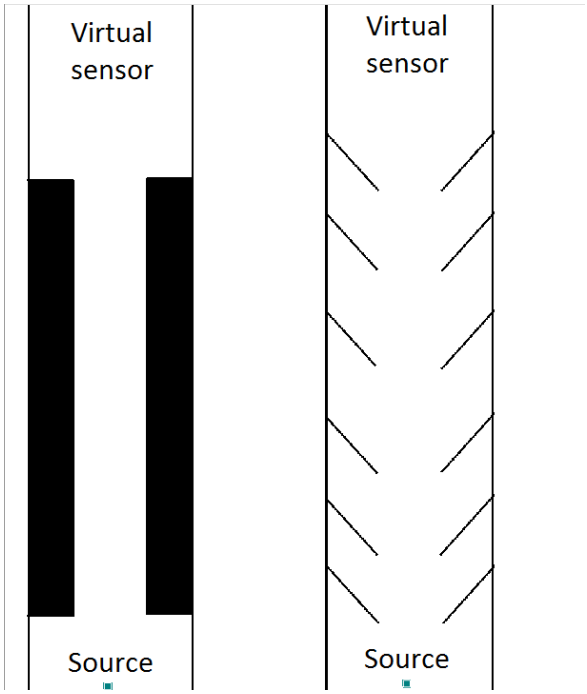

Figure i: A noise attenuation geometry concept tested in Falstad Ripple (Falstad) consisting of a series of diverging walls (right) and a control tube for comparison (left). Diverging tubes are said to cause attenuation due to an impedance mismatch between the inlet and outlet (Beranek, 1998).

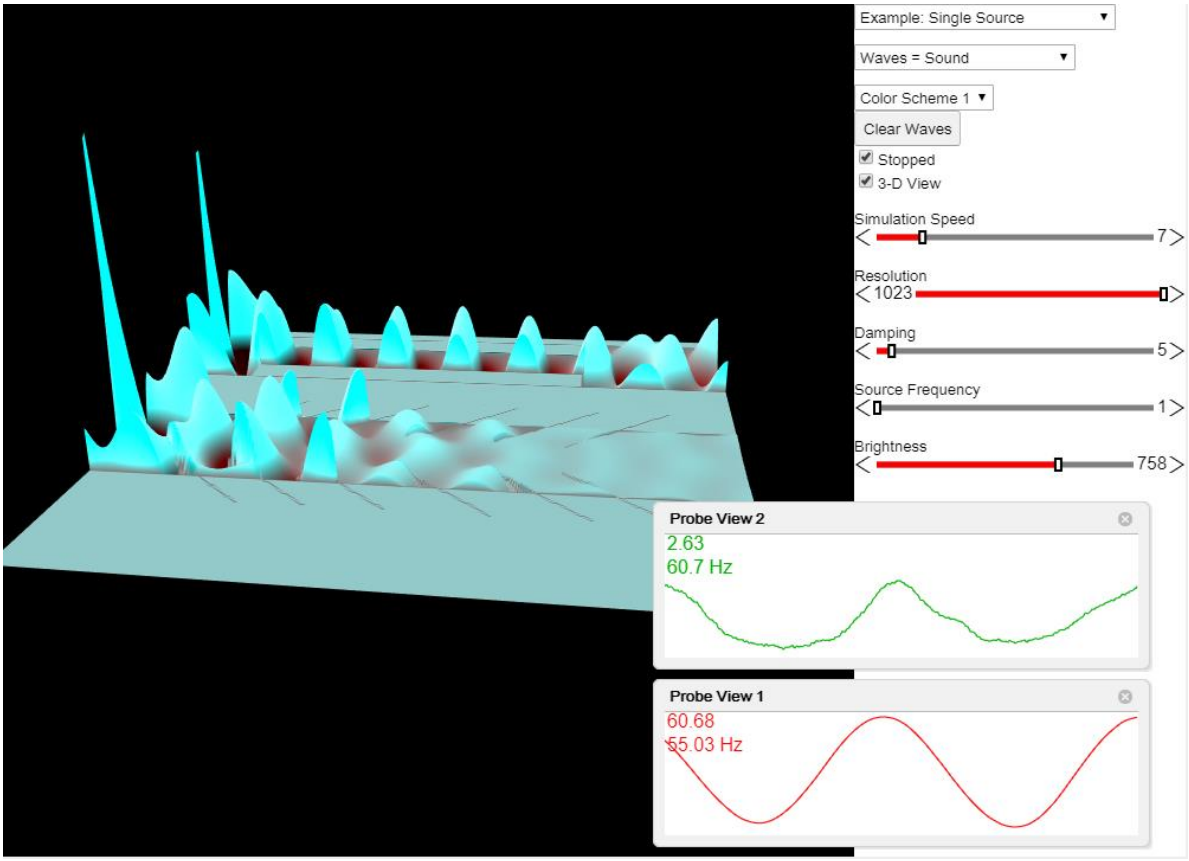

Figure j: The results of the Falstad Ripple (Falstad) simulation on the diverging geometry. Noise is reduced by over 95%, which is considered unrealistically optimistic. This is likely due to the overly simplified software.

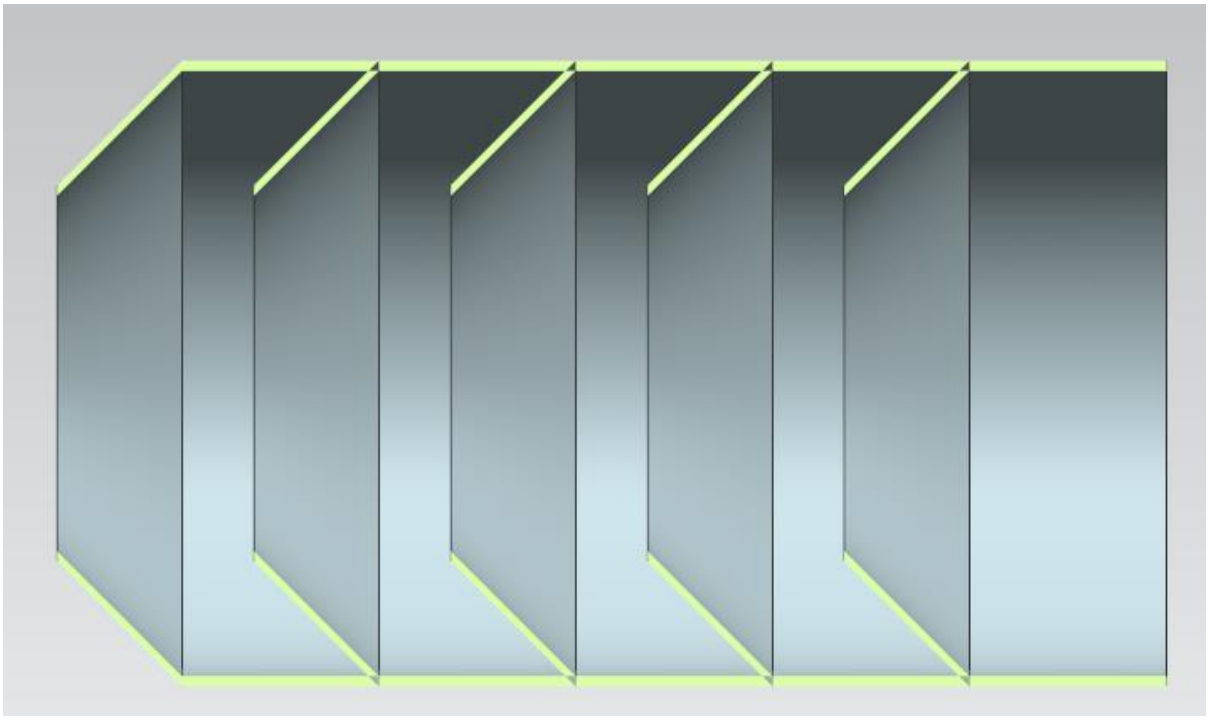

Figure k: CAD cross-section of the diverging series outlet concept. Unfortunately it was not manufactured for physical testing due to a combination of time constraints and lack of available materials.